



Surface plasmon resonance biosensors and their medical applications

Tomáš Špringer, Markéta Bocková, Jiří Slabý, Foozieh Sohrabi, Magdalena Čapková, Jiří Homola ^{*} 

Institute of Photonics and Electronics of the Czech Academy of Sciences, Chaberská 1014/57, 182 51, Prague, Czech Republic

ARTICLE INFO

Keywords:

Surface plasmon resonance biosensor
Plasmonic affinity biosensor
Optical biosensor
Medical diagnostics
Biomarker

ABSTRACT

Surface plasmon resonance (SPR) biosensors are an advanced optical biosensing technology that has been widely used in molecular biology for the investigation of biomolecular interactions and in bioanalytics for the detection of biological species. This work aims to review progress in the development of SPR biosensors for medical diagnostics, focusing mainly on advances in optical platforms and assays enabling analysis of complex biological matrices. Applications of SPR biosensors for the detection of medically relevant analytes, such as nucleic acids, proteins, exosomes, viruses, bacteria, and circulating tumor cells, are also reviewed. The detection performance of current SPR biosensors is discussed, and routes for improving performance and expanding applications of SPR biosensors in medical diagnostics are outlined.

1. Introduction

In modern medicine, diseases are frequently diagnosed and monitored based on the levels of biomarkers in bodily fluids. Biomarkers are a broad class of chemical and biological species that exhibit altered concentrations or functional characteristics associated with specific pathologies (Califf, 2018). In clinical laboratories, the levels of biomarkers (usually in blood or urine samples) are typically determined by enzyme-linked immunosorbent assay (ELISA), chemiluminescence immunoassay (CLIA), and polymerase chain reaction (PCR), depending on the nature of the particular biomarker (de Planell-Saguer and Rodicio, 2013; Turgeon, 2015). These methods enable the analysis of a high number of samples and are adapted to various biomolecules. However, they also exhibit limitations, such as laborious and time-consuming multi-step measurements, sample preparation, the need for trained staff, and expensive laboratory equipment. In addition, the conventional methods are typically confined to central laboratories, which results in delays between sample collection and results with a potential impact on clinical decisions and patients' well-being.

Affinity biosensors are an emerging technology with immense potential in medical diagnostics. Among them, surface plasmon resonance (SPR) biosensors are one of the most advanced label-free biosensing technologies (Homola, 2008). The first use of surface plasmons for probing processes on the surfaces of metal layers (Gordon and Ernst, 1980) and sensing (Nylander et al., 1982) was reported in the 1980s. In

1991, the first application of a surface plasmon-based sensor for the investigation of the interaction between biomolecules was described (Lofas et al., 1991). In the following years, SPR biosensors have become a "gold standard" for the real-time and label-free investigation of biomolecular interactions. In addition, SPR biosensors have been shown to be well-suited for the detection of various molecular biomarkers (Homola, 2008; Masson, 2017). Compared to other label-free methods, such as electrochemical and quartz crystal microbalance sensors (Alanazi et al., 2023; Zhang et al., 2023), SPR biosensors can provide high throughput measurements as well as visualize nano- and micro-scale objects near the sensor surface with temporal and spatial resolution and thus provide additional information of interest (Bocková et al., 2019). SPR biosensors have also been shown to hold vast potential for miniaturization, providing the path for the development of portable devices allowing analysis of biological samples outside the specialized laboratories (Lewis et al., 2021). The analysis of biological samples in a point-of-care setting shortens the time needed to obtain results. This enables prompt medical decisions and treatment, which improves the quality of a patient's life and reduces treatment costs.

In this review, we summarize the advances in the development of SPR biosensors for medical diagnostics, focusing on the period of the past seven years. Special attention is devoted to recent developments in optical platforms and detection formats and applications of SPR biosensors for the detection of medically relevant analytes, including nucleic acids, proteins, exosomes, viruses, bacteria, and circulating

^{*} Corresponding author.

E-mail address: homola@ufe.cz (J. Homola).

<https://doi.org/10.1016/j.bios.2025.117308>

Received 7 December 2024; Received in revised form 14 February 2025; Accepted 23 February 2025

Available online 24 February 2025

0956-5663/© 2025 Published by Elsevier B.V.

tumor cells (CTCs). In the review, we focus primarily on the publications that report on the detection of clinically relevant analytes in complex real-world samples.

2. Fundamentals of surface plasmon-based affinity biosensors

Optical affinity biosensors based on surface plasmons represent a diverse group of approaches that exploit special modes of electromagnetic field, surface plasmons (SPs), to measure refractive index changes associated with biological processes (e.g., interactions among biomolecules). While this basic principle remains the same for all such biosensors, they may differ in terms of the type of the plasmonic modes they employ (and by the type of the (nano)structure supporting SPs) and the method they use to optically excite and interrogate the plasmonic modes.

Two main classes of plasmonic modes used in biosensing include the so-called propagating surface plasmons (PSPs), typically supported by continuous metal layers or stripes, or the so-called localized surface plasmons (LSPs) supported by metal nanoparticle(s). The biosensors employing these two classes of modes are typically referred to as SPR biosensors (Homola et al., 2006; Schasfoort, 2017) or LSPR (localized surface plasmon resonance) biosensors (Mayer and Hafner, 2011; Willets and Van Duyne, 2007) or collectively, SPR biosensors. In recent years, various other plasmonic modes have been exploited in biosensors, including modes based on the coupling between different plasmonic modes (resonance coupling between propagating plasmons and localized plasmons in plasmonic nanoholes, Fano-like resonances of dark and bright modes of nanoparticle clusters, surface lattice resonances of a periodic array of nanoparticles), waveguiding effects (propagating plasmons in sparse nanoparticles, and plasmonic stripes), and others. A comprehensive list can be found in Špačková et al., 2016. The plasmonic modes may exhibit vastly different characteristics. One of the key characteristics is the profile of the electromagnetic field of the plasmonic mode, as it determines from what area the information about the refractive index changes is collected. This characteristic is often expressed in terms of the penetration depth, which may, depending on the type of plasmonic mode, vary from a few nanometers for highly localized modes to hundreds of nanometers or even microns for the delocalized long-range modes (Berini, 2009; Jatschka et al., 2016).

Biosensors based on surface plasmons employ the “resonance” between the incident light and SPs excited on metal or metal-dielectric (nano)structures. The efficient coupling between the light and SPs typically takes place within a narrow range of conditions, which are defined by the laws of energy and momentum conservation. The coupling condition, sometimes referred to as resonance condition, interrelates parameters of the system, the angle of incidence, and the wavelength of incident light that provide the strongest coupling. Therefore, the resonance can be observed as a characteristic feature (typically as a dip or peak) in the angular or wavelength spectrum of light coupled to SPs. These approaches are referred to as SPR spectroscopy in the angular or wavelength domain (or approaches based on angular or wavelength modulation). In addition, excitation of plasmonic modes can also be observed in the single angle of incidence and single wavelength configurations, in which changes in the intensity of light (inversely proportional to the strength of coupling) are observed. Sensors based on the measurement of changes in the light intensity are referred to as sensors based on intensity modulation and also include the so-called SPR imaging that is based on the intensity changes from an array of sensing spots (Wong and Olivo, 2014). Recently, the approach that combines data collection in a spatial domain with a spectral domain using a set of filters or a color camera has been developed and referred to as hyperspectral imaging (Mehta et al., 2021).

Various methods for the optical excitation of SPs have been developed and used. The most common method is based on the attenuated total reflection and a prism to couple light to SPs propagating on a continuous metal film. This technique has been combined with both SPR

spectroscopy and SPR imaging approaches and the corresponding optical platforms aimed to deliver the highest sensing performance. This technique has resulted in a variety of sensor instruments (including commercial systems) mostly for laboratory use. A prism may be replaced with a microscope objective that serves for both coupling and magnification of the imaged area, which leads to another approach referred to as SPR microscopy. The second most frequent method is based on the diffractive coupling of light to SPs on a metal grating. This method requires only simple optics and enables a higher degree of miniaturization. In addition to continuous metal films, various types of plasmonic modes have been excited on a multitude of nanostructures. In periodic nanostructures, diffractive coupling of collimated light into SPs has been widely used. Notably, periodic arrays of nanoholes were combined with spectrometry, imaging, and hyperspectral approaches (Ansaryan et al., 2023). This geometry provides the potential for high sensing performance, multiplexing, and miniaturization. In contrast to periodic structures, plasmonic modes on arrays of randomly distributed nanoparticles are typically excited by direct illumination, providing the advantage of simple read-out optics or even simple qualitative read-out by the naked eye (Yanik et al., 2011).

In SPR biosensors, the optical system for the excitation and interrogation of plasmonic modes is combined with other important elements to deliver the performance and features desired for a given application. These typically include functional coatings that provide the biosensor with a desired selectivity towards the specific analyte and the fluidic system that enables sample delivery to the sensor surface. Other elements may include temperature stabilization for robust performance in challenging environments or sample preparation units for sample extraction/preprocessing.

3. Advances in optical platforms

3.1. ATR-based optical platforms

Platforms based on the attenuated total reflection (ATR) are the most commonly used platforms in SPR biosensors. While most prism-based platforms employ continuous flat metal films to support PSPs, recently, they have been increasingly combined with structured plasmonic substrates supporting various SP modes with diverse characteristics. Arrays of plasmonic nanostripes supporting propagating modes (Slabý et al., 2021) and arrays of nanorods supporting localized modes (Špačková et al., 2018) have been combined with the ATR approach and optimized with respect to optical performance and analyte-collection effectivity and demonstrated to improve the bioanalytical performance by a factor of 2–7 when compared to traditional SPR biosensors. Nanorod dimers have been shown to be well suited for the detection of small analytes trapped in the most sensitive area – the dimer gap (Portela et al., 2020) and the nanorod-dimer-based biosensor was shown to be able to detect sub-nM concentration of microRNA (miR). The 1D structure based on the gold and gold-ZnS-Ag layers was investigated by Lee et al. (2018), who showed that although the conventional approach with a flat gold film provided higher performance in the angular modulation mode, the gold-ZnS-Ag multilayer provided better performance in the intensity modulation mode. In another work, a double layer of metal and silicon thin films was shown to increase the penetration depth of an SP mode and improve the figure of merit of the sensor in the wavelength modulation mode (Shrivastav et al., 2021).

3.2. Microscopy-based optical platforms

Optical platforms based on plasmonic microscopy use a microscope objective to couple and collect light from a plasmonic substrate. Plasmonic microscopy is used primarily for imaging at a single wavelength (as such an approach allows for more straightforward instrumentation when compared to spectroscopy) or for microspectroscopy using either fiber-based or imaging spectrometers or color-sensitive cameras with

appropriate data processing.

As LSPs can be excited on metal nanoparticles directly without the use of any coupling device, metal nanoparticles are a natural choice for plasmonic microscopy. Metal nanoparticle arrays can be easily fabricated by anodic annealing (Ma et al., 2022) and integrated within automated microfluidic systems (Chen et al., 2020). An interesting work was published by Sperling et al., who combined the nanoparticle array with microspectrometry for self-referenced optical sensing (Sperling et al., 2018). They used nanoparticles with the bare surfaces for sensing, and nanoparticles embedded within a resist as a reference and demonstrated that this approach allows for the reduction of the baseline drift. Raghu et al. combined an array of metal-coated pillars with an optical system with $100\times$ magnification and a digital detection approach (Raghu et al., 2018). The image of the whole array was recorded and signals from individual pillars were analyzed. While the attachment of a larger object (exosome) to a pillar was registered as a distinct jump in the light intensity, the attachment of a smaller object (protein) produced negligible sensor response. Various plasmonic sensors based on nanohole arrays and microscopy have been reported. Altug et al. employed gold nanohole arrays with a compact optical system that consisted of a light-emitting diode (LED) that matches the wavelength of extraordinary optical transmission, an objective, and a complementary metal–oxide–semiconductor (CMOS) camera to detect the gold nanoparticles (AuNPs) bound to a single nanohole (Belushkin et al., 2018, 2020). In another approach, a nanohole array was placed on a thin membrane, forming a stacked multilayer including two gold layers, one of which was perforated with nanoholes (Tu et al., 2019). It was demonstrated that a dielectrophoretic preconcentration of the analyte allowed for a 6-fold improvement in the sensing performance. An SPR microscopy exploiting a gold film with nanoparticles was reported by Chen et al. (2018). Their approach used a coaxial dual-objective microscope to record two different types of images – the SPR microscopy image and the image of light scattered on nanoparticles. Based on the analysis of the two images in real time, the nanoscale amplitude of oscillation of the nanoparticle was retrieved, and the statistical analysis showed that the variations correlate with the level of hybridization of miR located between the nanoparticle and substrate. The approach was shown to be able to detect the single nucleotide polymorphisms in miR.

3.3. Free-space optical platforms

Free-space optical platforms usually employ collinear arrangements for imaging at a single wavelength or multiple wavelengths using spectroscopy. These optical platforms have been used with various types of plasmonic substrates, from gratings and slits to arrays of nanoparticles.

Various configurations of plasmonic sensors based on diffraction gratings have been developed. Nair et al. reported a compact optical sensing platform based on plasmonic crossed diffraction gratings and integrated 3D-printed units with an LED and a CMOS camera (Nair et al., 2020). Diffraction gratings replicated into polyethylene terephthalate were used in another collinear sensor platform (Baek et al., 2020). In another work (Fan et al., 2020), a diffraction grating was combined with a simple read-out using an LED, microlenses, and polydimethylsiloxane-based fluidics to form a compact sensor device. Gratings based on blue-ray discs were utilized in another collinear system employing a fiber-coupled spectrometer (Lopez-Munoz et al., 2020).

Plasmonic nanohole arrays have also been widely combined with free space optics. Cetin et al. reported a handheld device based on the nanohole array and demonstrated its use for the detection of viruses (Cetin et al., 2021). Another approach utilized bio-printed microarrays on gold nanohole substrates and a portable lens-free interferometric microscopy platform for the detection of bacteria (Dey et al., 2019). A gold nanohole array was also used for the construction of a sandwiched plasmon ruler that exhibited enhanced sensitivity due to the plasmonic coupling effect (Nan et al., 2020). Nanohole array and photonic

crystal-based biosensors employing spectroscopy in visible- and near-infrared spectroscopy were compared by Cetin et al. (Cetin and Topkaya, 2019).

Plasmonic slits were combined with an optical platform based on surface-plasmon interferometry (Kuo et al., 2022). This sensor employed a gold film with gold caps supporting Fano resonance. The attachment of biomolecules between the caps produced a change in the strength of Fano resonance and resulted in a change in the resonant feature in the spectrum. This approach was shown to provide better performance than an SPR biosensor using a thin gold film. SP interference on Al nanoslits was used by Hsieh et al., who developed a biosensor for the detection of viruses (Hsieh et al., 2022). They successfully combined the biosensor with analyte preconcentration using an electrochemical effect on a Nafion membrane deposited on the sensing structure. Another sensing platform based on plasmonic interference on nanocup arrays and intensity interrogation was developed and tested for the detection of cancer biomarkers (Hackett et al., 2018). In the follow-up work, the device read-out was modified to support two wavelengths and a microplate reader, and the platform was used for the detection of viruses (Fan et al., 2022). Liang et al. demonstrated that a highly ordered gold nanodisk array on opaque gold film can support two distinct modes: surface-plasmon-polariton and Bloch mode (Liang et al., 2019). The authors used the Bloch mode to detect proteins with a limit of detection (LOD) better by an order of magnitude when compared to prism-based commercial SPR sensors. Another approach using nanocup arrays was proposed by Liu et al., who combined the array with AuNPs to enhance response in UV spectroscopy and used the sensing platform for the detection of miR (Liu et al., 2023). A plasmonic sensor platform based on large-area gold nanocheckerboard metasurfaces on flexible plastics was reported by Cai et al. (2019). Zopf et al. reported a plasmonic sensor based on AuNPs deposited on (3-aminopropyl)triethoxysilane (APTES)-modified glass surface (Zopf et al., 2019). The spectrum of light coupled with the array of AuNPs was recorded by Fourier-transform imaging spectrometry and the platform was used for the multiplexed detection of DNA.

Various groups reported the development of smartphone-based platforms. In (Zhang et al., 2022), the continuous gold film was combined with standard components (a prism and a flow cell) and a smartphone into a compact setup. An intensity-based interrogation approach was shown to enable simultaneous measurement in 12 independent sensing spots. Using a smartphone camera, Bian et al. developed a sensor based on a plasmonic array in which the unit structures had varying sizes, giving rise to a shift in plasmonic resonance along the array (Bian et al., 2019).

3.4. Integrating optics and microfluidics

In recent years, various attempts to integrate structures supporting SPs with microfluidic devices have been reported. Liu et al. used a capillary with its inner wall modified with gold NPs used in conjunction with an optical system recording both scattered and transmitted light (Liu et al., 2019). Another approach aimed at improving analyte transport towards the sensor surface exploiting flow through a plasmonic substrate with a vertical nanorod antenna array (Klinghammer et al., 2018). The optofluidic device was evaluated for the detection of hybridization of short oligonucleotides. Yavas et al. have developed a microfluidic chip integrated with nanoplasmonic arrays (Yavas et al., 2018). The networks of microfluidic channels allowed for the precise handling of liquid samples toward an array of gold nanorods. The device was tested for the detection of cancer protein biomarkers.

3.5. Summary

Historically, biosensors based on surface plasmons have mostly utilized the configuration based on the ATR method. Although this trend continued even in the last decade, the ATR method has been increasingly

combined with nanoparticles and nanostructures that support a variety of plasmonic modes. The ATR sensing platforms employing thin metal films have been investigated and, through systematic long-term effort, advanced to the level of performance that is given by the physical limits (noise). Therefore, improvements in the detection performance of biosensors based on surface plasmons are now achieved mainly through the use of plasmonic nanostructures and optimization of their optical and mass transport characteristics. Furthermore, optical platforms based on plasmonic microscopy are increasingly exploited to allow for localized measurements, which also include the acquisition of sensing responses from individual nanoparticles and digital detection. The microscopy platforms thus may allow for sensing in a large number of miniature spots, reducing the consumption of expensive chemicals and, thus, the cost of the analysis in routine clinical practice. Another trend in the development of optical platforms regards the simplification of optics and, thus, the reduction of instrumentation costs. Herein, approaches based on free-space collinear optics to excite SPs on nanoparticles and nanostructures play an important role and have been demonstrated to provide an avenue for the construction of compact devices suitable for point-of-care diagnostics. These developments are accompanied by advances in the integration of plasmonic structures with microfluidic structures into optofluidic platforms.

4. Advances in detection formats

Clinical samples contain large and diverse populations of molecules that may interfere with biosensor-based detection of analytes and produce false positive sensor responses due to the nonspecific binding of such molecules to a sensor surface. In addition, the concentration of analyte molecules is usually very low compared to the concentrations of the most abundant molecules in clinical samples. To address these challenges, various detection formats have been developed to boost specific sensor response (due to the analyte) and suppress the nonspecific binding from complex biological matrices.

One of the most widely used detection formats is a sandwich assay in which the specific sensor response is enhanced by functionalized metal nanoparticles, such as spherical AuNPs (Sguassero et al., 2019) or nanorods (Kim et al., 2018), Ag nanocubes (Wu et al., 2021), spherical core/shell $\text{Fe}_3\text{O}_4/\text{Au}$ nanoparticles (Premaratne et al., 2019), or biological nanoparticles, such as receptor-coated liposomes (Akkilic et al., 2019). As the enhancing step with the nanoparticles is performed in simple solutions (e.g., buffers), the specific sensor response is significantly enhanced by nanoparticles, while the nonspecific sensor response is enhanced significantly less (Špringer et al., 2017). Recently, various modifications of a sandwich assay have been proposed. Lim et al. used a combination of a sandwich assay and two enzymatic reactions for the detection of protein secretogranin II (SCG2) (Lim et al., 2021). A sandwich complex containing primary antibody, SCG2, biotinylated

secondary antibody, and streptavidin-horseradish peroxidase conjugate was initially formed on a sensor surface. Then, the tyramide reaction was used to biotinylate close proteins around the formed sandwich complex. Finally, streptavidin-alkaline phosphatase was bound to biotinylated proteins and used to form an insoluble precipitate from substrate molecules introduced in the solution (Fig. 1). The sedimentation of the precipitate served as the final enhancement step, and an LOD of 16 pg/mL was demonstrated in 10% blood serum. Špringer et al. proposed a novel nanoparticle release assay to detect nucleic acids (Špringer et al., 2021). In this approach, the sensor surface was functionalized with oligonucleotide probes, followed by the capture of the target miR and oligonucleotide-modified AuNPs. Subsequently, the specifically bound oligonucleotide-AuNPs were released using a displacing DNA sequence. This assay enhanced only the specific sensor response (due to the target miR) while suppressing the interfering effects caused by the non-specific binding. It enabled the detection of miR at sub-fM level in 10% blood plasma.

Detection formats employing nuclease enzymes have also been reported. Chen et al. combined a DNA walking system with an enzymatic cleavage reaction to detect miR-182 (Chen et al., 2022). Two oligonucleotide probes (a short biotinylated probe and a long probe partially blocked by a short complementary strand) were immobilized on a sensor surface. The target miR bound to the short complementary strand, which released the long probe for hybridization with the short biotinylated probe immobilized on the sensor surface. Then, the short biotinylated probe in the formed duplex was cleaved by sequence-specific endonuclease. Finally, the long probe was released and hybridized with another short biotinylated probe. The repeated hybridization/cleavage cycles resulted in a decrease in the surface density of biotin, which was quantified in the last step of the assay. The final sensor response was shown to be indirectly proportional to the concentration of target miR with a linear detection range of 5–1000 fM, and the sensor was used to detect the target miR-182 in filtered 20% serum. Huang et al. detected miR-21 using duplex-specific nuclease (DSN) (Huang et al., 2021). The sample (cell lysate from MCF-7 or HeLa cancer lines) was mixed with the oligonucleotide DNA probe, which was biotinylated on both ends and complementary to the target miR-21. The DSN enzyme specifically cleaved the DNA probe in the formed hybrid miR-21/probe duplex, and miR-21 was released to form a duplex with another DNA probe. The repeated hybridization/cleavage cycles decreased the concentration of DNA probes containing two biotins. The mixture solution was injected along a streptavidin-coated sensor surface to allow the capture of the biotinylated probes. In the last step, the sensor response was enhanced by the binding of streptavidin-AuNPs to the second biotin on the captured non-cleaved probe. An LOD as low as 1 fM was demonstrated using this approach.

As structural and functional changes in proteins can serve as biomarkers in certain pathologies, assays to assess changes in proteins have

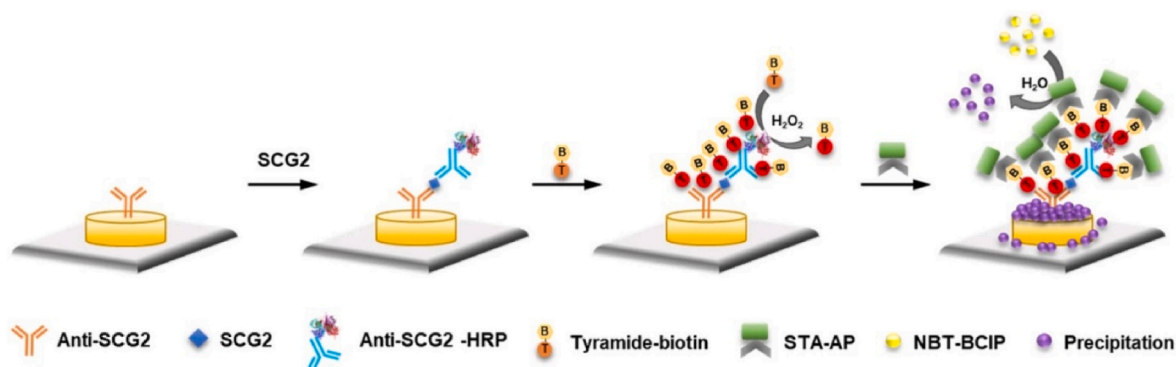


Fig. 1. Multi-step sandwich assay using two enzymatic reactions and formation of precipitate for the detection of SCG2 protein. Reprint with permission from (Lim et al., 2021).

also been developed. Pastva et al. developed an assay to quantify the misfolded proteins in blood plasma (Pastva et al., 2019). A sensor surface was modified with heat shock protein 70 (Hsp70) that captures misfolded proteins in the presence of ADP and releases them in the presence of ATP. Misfolded proteins were captured from 10% plasma and subsequently eluted in buffer and identified using liquid chromatography with tandem mass spectrometry. The analysis of clinical plasma samples showed a significant increase in the concentration of misfolded proteins in certain stages of myelodysplastic syndromes (MDS). An interatomic approach was proposed by Chrástíková et al. (2019). In this approach, the sensor surface was modified with six different proteins relevant to MDS and a blood plasma sample was injected along the sensor surface. The binding of unknown plasma components to the attached proteins was recorded using an SPR imaging sensor. The approach was demonstrated to distinguish MDS patients from healthy controls as well as differentiate among MDS subtypes.

5. Detection of biomarkers

SPR biosensors have been applied to detect a variety of biological species related to human health, ranging from nucleic acids and proteins to viruses, bacteria, and CTCs.

5.1. Nucleic acids

5.1.1. RNA

Simultaneous detection of four miRs relevant to multiple sclerosis (miR-422, miR-223, miR-126, and miR-23a) was reported by Squassero et al. (2019). They used thiolated DNA probes microspotted onto an SPR imaging sensor surface, and polyA DNA was applied to block the remaining surface. Detection of miRs in buffer was performed using a sandwich assay with neutravidin-coated AuNPs functionalized with an antibody against DNA/RNA hybrids, and LODs ranging from 0.55 to 1.79 pM were attained. The clinical applicability of the approach was evaluated by quantifying the target miRs in the total RNA extracted from human blood serum. The results obtained by the biosensor showed a good agreement with the reverse transcription PCR. Simultaneous detection of diabetic neuropathy-associated miRs (miR-21, miR-192) was performed by Wei et al. (2018). They used an SPR imaging platform with a flat gold sensor surface functionalized with thiolated DNA probes and an enhancement strategy based on a sandwich assay combining strand displacement amplification (SDA) and DNA-functionalized AuNPs. The SDA analyte enrichment was performed *ex-situ*, where the miRs specifically hybridized with the corresponding hairpin probes and initiated the SDA, resulting in a massive production of trigger DNA. After the SDA step, the solution was injected over the sensor surface and the trigger DNA hybridized with the immobilized probes and DNA-functionalized AuNPs, assembling a DNA sandwich complex. This approach achieved LODs down to 0.15 pM for miR-21 and 0.22 pM for miR-192 in buffer. The clinical potential of the proposed assay was verified in 10% fetal bovine serum with a good recovery (~105%). The same group employed an SPR imaging sensor for the simultaneous detection of exosomal miRs (miR-21, miR-378, miR-139, and miR-200) associated with non-small cell lung cancer (NSCLC) (Wu et al., 2021). The gold surface was functionalized with various thiolated DNA tetrahedral frameworks to capture the target miRs. DNA-functionalized silver nanocubes (AgNCs) were injected to hybridize with the captured miRs. Then, the DNA-coated AuNPs assembled on the surface of AgNCs, forming Au-on-Ag heterostructures and providing a sensor response enhancement. The developed biosensor was applied to the detection of miRs extracted from clinical samples and demonstrated to allow for the discrimination of NSCLC patients from healthy controls. Premaratne et al. proposed an SPR imaging biosensor for the combined detection of oncologically relevant proteins (IL-6, IL-8) and miRs (miR-21, miR-155) (Premaratne et al., 2019). The individual spots on the sensor surface were functionalized with anti-IL antibodies and

thiolated DNA hairpin probes. The detection of miR was performed in 10% human blood serum using a sandwich assay with Fe₃O₄/AuNPs functionalized with secondary antibodies or DNA. LODs of 28, 18, 0.5, and 0.48 pM in 10% plasma were measured for IL-6, IL-8, miR-21, and miR-155, respectively. Springer et al. used a six-channel SPR biosensor to detect miR-125b and miR-16, potential biomarkers of myelodysplastic syndromes (Springer et al., 2021). The nanoparticle release assay was used to detect miR-125b and miR-16 in 10% blood plasma samples with LODs of 350 and 550 aM, respectively. The method was applied to detect miR-16 in plasma samples of patients with myelodysplastic syndromes. Chen et al. used a commercial SPR biosensor to detect miR-182 associated with glioma tumors (Chen et al., 2022). The assay combining the DNA walking system with the enzymatic cleavage reaction enabled the detection of miR-182 with an LOD of 620 aM in buffer. The biosensor was applied to the analysis of clinical samples (blood serum). It was demonstrated that the serum of glioma patients exhibited ~3 times higher miR-182 levels than the serum from healthy controls.

5.1.2. DNA

Breviglieri et al. reported an SPR biosensor for the detection of four different thalassemia-related point mutations of the human beta-globin gene (Breviglieri et al., 2018). The specifically designed biotinylated DNA probes were attached to the streptavidin-coated flat gold surface. Two DNA probes differing in a single base, one complementary to the normal sequence and the other to the mutated one, were immobilized on a sensor chip and captured the genomic DNA, which was previously amplified by PCR. The ratio of the signal generated by the interaction of the sample with different DNA probes was evaluated to differentiate among healthy individuals, heterozygous thalassemia carriers, and homozygous thalassemia patients in over 70 blood and saliva swab samples. Calvo-Lazano et al. developed an SPR biosensor to diagnose pneumocystis pneumonia (Calvo-Lozano et al., 2020). Their approach was based on the poly-purine reverse-Hoogsteen hairpin probes for the detection of the DNA coding mitochondrial large subunit ribosomal RNA in *Pneumocystis jirovecii*. A mixture of thiolated DNA hairpin probes and HS-PEG-CH₃ was chemisorbed onto a flat gold surface, followed by a sample injection. The target DNA formed an antiparallel triplex structure with a hairpin probe, enabling stronger capture of the target DNA than the traditional approach based on duplex hybrids through linear DNA probes. The approach provided an LOD of 2.1 nM in buffer. Then, the authors analyzed clinical samples (DNA extracted from bronchoalveolar lavages or nasopharyngeal aspirates from four samples positive for *P. jirovecii* and eight control samples positive for two other different microorganisms (i.e., *Pseudomonas* and *Cladosporium*). It was shown that the biosensor could discriminate clinical samples of patients infected with *P. jirovecii* from samples infected with other microorganisms.

SPR biosensors can also detect circulating tumor DNA (ctDNA). D'Agata et al. developed an SPR biosensor for the simultaneous detection of eleven selected single-point rat viral sarcoma oncogene (RAS) mutations, which are known to be associated with primary or acquired resistance to antibodies to epidermal growth factor (EGFR) treatment of colorectal cancer patients (D'Agata et al., 2020). Amine-terminated peptide nucleic acid (PNA) probes, which were complementary to mutated or wild-type RAS, were covalently attached to a flat gold surface of an SPR imaging sensor functionalized with dithio-bis-succinimidyl propionate. The detection was based on a DNA sandwich assay using DNA-functionalized AuNPs. The assay could discriminate between wild-type and mutated ctDNAs in 10% blood plasma samples down to a ctDNA concentration of 2 ng/mL. The biosensor enabled discrimination between colorectal cancer patients and healthy volunteers. Bellassai et al. used the commercial SPR imaging sensor to detect Kirsten rat viral sarcoma (KRAS) oncogene mutations (Bellassai et al., 2021). The sensor surface was functionalized with PNA probes complementary to mutated or wild-type KRAS. The target DNA was captured by the respective PNA probes and the sensor response was

enhanced using DNA-functionalized AuNPs. The detection of wild-type and mutated KRAS ctDNAs was performed in 10% blood plasma with an LOD of 1.45 ng/mL. The biosensor enabled to discriminate between a colorectal cancer patient and a healthy donor. The use of LSPR modes on differently shaped nanoparticles for the detection of mutated KRAS was studied by Tadimety et al. (2021). Gold nanorods, nanospheres, and nanobipyramids were functionalized with PNA probes complementary to the mutated KRAS. The nanobipyramids provided the best performance enabling the capture of ctDNA at the ng/mL range in blood serum.

5.2. Proteins

5.2.1. Cancer biomarkers

Lee et al. used the commercial SPR biosensor Biacore 3000 to detect heterogeneous nuclear ribonucleoprotein A1 (hnRNP A1) (colorectal cancer) (Lee et al., 2020). The sensor surface was functionalized with aptamers against hnRNP A1, and a sandwich assay with a secondary antibody was used to enhance the assay's sensitivity. This approach was demonstrated to allow the detection of hnRNP A1 at nM levels in buffer and blood plasma samples. Yang et al. used the commercial SPR biosensor, Biacore T200, to detect interleukin 2 (IL-2) and soluble IL-2 receptor (sIL-2R α) proteins (myeloma cancer) (Yang et al., 2021). They modified the sensor surface with bioresponsive microgels incorporating IL-2/sIL-R α receptors. The proteins IL-2 and sIL-2R α present in the sample formed a multi-complex with the immobilized receptors. The SPR sensor response enabled the detection of IL-2 and sIL-2R α at concentrations down to ~ 20 nM. By analyzing the diluted blood serum samples of cancer patients, the authors observed elevated levels of IL-2 and sIL-2R α compared to healthy controls. Yang et al. reported the detection of three bladder cancer biomarkers - nuclear matrix protein 22 (NMP22), human complement factor H (CFH), and hyaluronic acid (HA) (Yang et al., 2023). They used an LSPR biosensor with gold nanomushrooms modified with respective antibodies via amino-coupling and a sandwich assay with AuNPs to enhance the sensitivity of the assay. The biomarkers present at ng/mL and sub-ng/mL levels were measured in

buffer and 10% fetal bovine serum samples. The multiplexed detection of four proteins (CA 15-3, CA 125, CEA, and ErbB2) related to breast cancer was reported by Yavas et al. (2018). They used an LSPR biosensor with a microfluidic cartridge (Fig. 2) and antibodies attached to a sensor surface via amino-coupling. Using a sandwich assay with secondary antibodies, LODs of CA 15-3, CA 125, CEA, and ErbB2 in human blood serum were established to be 1.85 U/mL, 1.021 kU/mL, 76.19 ng/mL and 31.9 ng/mL, respectively. Pastva et al. used an SPR biosensor to detect misfolded proteins related to MDS (Pastva et al., 2019). The developed assay revealed elevated levels of misfolded proteins in the two stages of MDS (low-risk (RARS) and intermediate-risk (RCMD)) that are most affected by oxidative stress. Neuron-specific enolase (NSE) and progastrin-releasing peptide (31–98) (ProGRP31-98), connected to small cell lung cancer, were detected by Sun et al. (2021). They used the commercial Biacore X100 SPR instrument and aptamers as bio-recognition elements. They performed direct detection of NSE and ProGRP31-98 in buffer with LODs of 3.9 nM and 15.6 nM, respectively.

5.2.2. Cardiovascular biomarkers

Palladino et al. used the commercial SPR biosensor Biacore XTM to detect troponin T (TnT) (acute myocardial infarction) (Palladino et al., 2018). The sensor surface was modified with a molecularly imprinted polymer (MIP) based on polydopamine. The authors detected TnT in buffer directly with an LOD of 14.8 nM. A sandwich assay with a secondary antibody was shown to allow for the detection of a sub-nM concentration of TnT in filtered human blood serum. Zhao et al. used an SPR sensor based on the Kretschmann configuration to detect a biomarker of heart failure - B-type natriuretic peptide (BNP) (Zhao et al., 2019). The solution containing BNP was mixed with antibody-coated magnetoplasmonic nanoparticles and aptamer-coated AuNPs. The formed BNP-nanoconjugate was captured on a DNA-modified sensor surface via the DNA-DNA interaction. The detection experiments were performed in buffer and levels of BNP used in these experiments ranged from 0.1 pg/mL to 10 ng/mL.

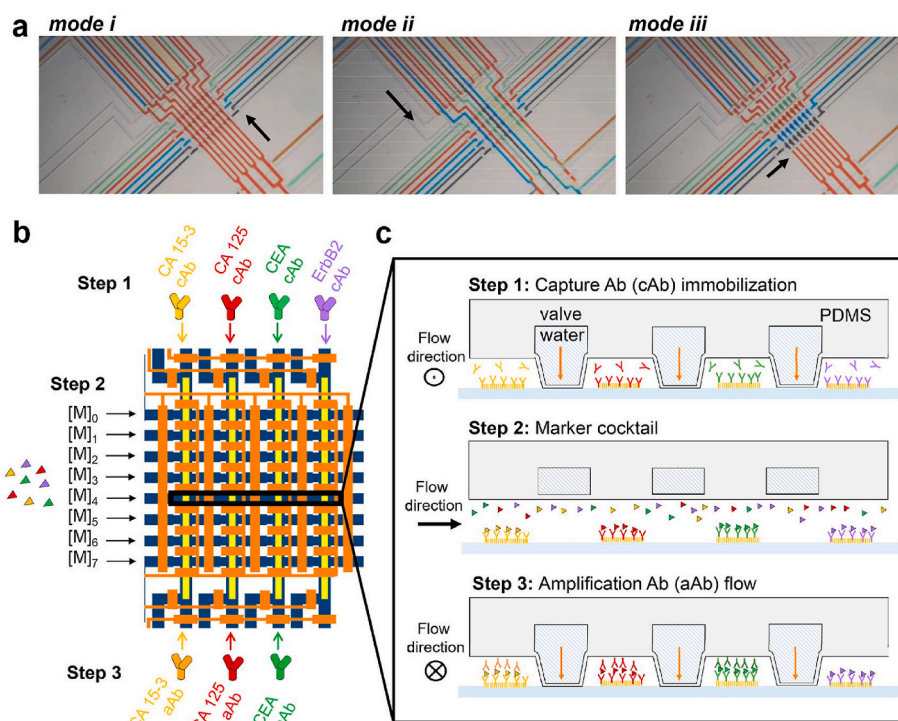


Fig. 2. SPR biosensor for multiplexed detection of cancer biomarkers. (a) Images of the microfluidic cartridge in different regimes. (b, c) Design of the experiment. Reprinted with permission from (Yavas et al., 2018). Copyright 2018 American Chemical Society.

5.2.3. Biomarkers of neurodegenerative diseases

Kim et al. developed a multiplexed LSPR biosensor to detect biomarkers of Alzheimer's disease - two beta-amyloid proteins ($A\beta_{1-40}$, $A\beta_{1-42}$) and protein τ (Kim, H. et al., 2018). Three AuNPs with different shapes (spheres, short rods, and long rods) were functionalized with respective antibodies against $A\beta_{1-40}$, $A\beta_{1-42}$, and τ via amino-coupling and attached to a glass substrate. Then, the proteins were directly detected in blood plasma. In the follow-up publication (Kim et al., 2019), Kim et al. detected protein τ in human blood plasma samples and observed elevated levels of τ in samples of Alzheimer's disease patients when compared to healthy controls. Nangare et al. developed a graphene-oxide decorated SPR biosensor to detect $A\beta_{1-42}$ (Nangare and Patil, 2022). The sensor surface with a gold layer was coated with graphene oxide and conjugates of silver nanoparticles and antibodies, and $A\beta_{1-42}$ was directly detected. It was revealed for Alzheimer's disease-induced animals that their cerebrospinal fluids contained higher levels of $A\beta_{1-42}$ than the blood or saliva samples. Antibodies against gangliosides, which are biomarkers of multiple sclerosis, were detected by Malinick et al. (2020). They used a prism-based SPR imaging biosensor coated with a thin layer of SiO_2 and a perfluorodecyltrichlorosilane layer. Three gangliosides (GA_1 , GM_1 , and GT_{1b}) mimicking the myelin sheath were adsorbed to the silane layer. Antibodies against GA_1 , GM_1 , and GT_{1b} were directly detected in buffer with LODs of 17.6, 11.3, and 8.2 ng/mL, respectively. Lim et al. reported an LSPR biosensor with gold nanodots for the detection of SCG2 - a potential biomarker of neurodevelopmental disorders (Lim et al., 2021). The developed assay was used to detect SCG2 with an LOD of 16 pg/mL in 10% blood serum. In addition, elevated levels of SCG2 were found in patient samples when compared to healthy controls.

5.2.4. Biomarkers of other diseases

Zhang et al. developed a smartphone-based SPR imaging biosensor to detect three acute kidney injury biomarkers (neutrophil gelatinase-associated lipocalin (NGAL), interleukin-18 (IL-18), and retinol-binding protein (RBP)) (Zhang et al., 2022). Different areas of the sensor surface were functionalized with respective antibodies against these biomarkers. A sandwich assay employing antibody-coated magnetic nanoparticles was used to detect NGAL, IL-18, and RBP in 50% urine with LODs of 0.19, 0.51, and 0.7 ng/mL, respectively. Zhang et al. detected four proteins (human serum albumin (HSA), kappa light chain (κ), lambda light chain (λ), and beta-2-microglobulin (B2M)) related to kidney diseases (Zhang, L.L. et al., 2022). They used a portable prism-based SPR biosensor and antibodies attached to the BSA-modified sensor via amino-coupling. HSA, κ , λ , and B2M were directly detected at levels down to 0.36, 0.05, 0.1, and 0.04 μ g/mL, respectively. They also demonstrated that urine samples of nephrotic patients exhibited elevated levels of all targeted proteins compared to the healthy controls. Shen et al. developed a prism-based SPR imaging biosensor to monitor peanut allergy by detecting allergen-specific immunoglobulin E (IgE) (Shen et al., 2018). Initially, IgEs were extracted from blood serum samples using antibody-coated magnetic particles (MP). Then, the extracted IgE-MP mixture was pumped along the sensor containing areas with different peanut epitopes. An LOD was established to be 5 pg/mL. The biosensor was also shown to differentiate the IgE levels in individuals having negative and positive levels of IgE against Ara h2 epitope of the major peanut allergen glycoprotein. Pelaez et al. used a prism-based SPR biosensor to detect gluten immunogenic peptides (GIP), small peptides derived from gluten digestions, to monitor gluten intake (Pelaez et al., 2020a). They used the competitive immunoassay, in which prolamins working group gliadin, a compound similar to GIP, was immobilized on the sensor surface and competed with GIP for the binding of the specific antibody. The authors reported an LOD of 1.6 ng/mL in undiluted urine and validated their method by analyzing urine samples of healthy volunteers with high recovery values (96–101%).

5.2.5. Proteins indicating viral or bacterial infection

SPR biosensors were also applied to detect viral and bacterial proteins to monitor infectious disease progression. Widoretto et al. used a commercial SPR biosensor NaviTM 220A NAALI to diagnose dengue, an acute febrile disease (Widoretto et al., 2020). An antibody against the viral nonstructural protein (NS1) was attached to a gold layer via a carboxy-dextran matrix. Direct detection was used to identify all 16 dengue-positive blood plasma samples and 10 controls, while ELISA and lateral flow assay used as reference methods exhibited several false-positive and false-negative results. Lewis et al. used a portable LSPR biosensor to detect the S1 spike protein of SARS-CoV-2 in buffer and artificial saliva (Lewis et al., 2021). A sensor surface was functionalized with streptavidin and biotinylated aptamer against the S1 spike protein. The biosensor was able to directly detect S1 spike protein in buffer with an LOD of 0.26 nM. Moreover, the authors demonstrated that the biosensor does not exhibit cross-reactivity with receptor binding domain (RBD), S2 spike protein, and BSA. Bhalla et al. reported an LSPR biosensor for the detection of Alpha, Beta, and Gamma SARS-CoV-2 variants (Bhalla et al., 2022). They used nanostructured MIPs and detected directly all variants in blood serum samples. Pelaez et al. used a prism-based SPR biosensor for the diagnostics of *Mycobacterium tuberculosis* (Mtb) infection (Pelaez et al., 2020b). Antibody against heat shock protein X (HspX), a biomarker of Mtb, was attached to a sensor surface via amino-coupling. HspX was detected directly in pretreated 50% sputum with an LOD of 0.6 ng/mL. In addition, elevated levels of HspX were found in sputum samples of patients with tuberculosis when compared to patients with other respiratory illnesses.

Besides the viral and bacterial proteins, much attention was given to antibodies and interleukins produced by the infected organism, which can also indicate the progression of infectious diseases. Due to the SARS-CoV-2 pandemic, many publications focused on the detection of antibodies against SARS-CoV-2. Funari et al. used an LSPR biosensor to detect antibodies against SARS-CoV-2 spike proteins (Funari et al., 2020). The sensor surface with gold nanospikes nanostructures was modified with the C-terminal peptide of SARS-CoV-2 spike protein via amino-coupling. The antibodies against SARS-CoV-2 were detected directly at the ng/mL range in buffer and diluted human blood plasma (1:1000). Antibodies against SARS-CoV-2 spike protein were also detected by Qu et al. (2022). They used a fiber optic SPR biosensor and receptor binding domain (RBD) of SARS-CoV-2 spike protein as a bio-recognition element (immobilized to the sensor surface via His-tag). A sandwich assay with antibody-coated AuNPs was used to detect the antibodies in diluted human blood serum and blood of SARS-CoV-2 patients at ng/mL levels. Calvo-Lozano et al. (2022) used a homemade prism-based SPR biosensor to detect antibodies against viral nucleocapsid (N) protein and receptor-binding domain (RBD) of the spike protein. A sensor surface was coated with both proteins (individual or in the mixture) via amino-coupling. Antibodies against N and RBD in 10% blood serum were detected directly with an LOD of 86 and 21 ng/mL, respectively. The approach was also used to differentiate between SARS-CoV-2-positive and SARS-CoV-2-negative samples ($n = 120$) with high diagnostic sensitivity (99%) and specificity (100%). Schasfoort et al. used the SPR biosensor technology to quantify IgG, IgM, and IgA antibodies against RBD (Schasfoort et al., 2021). They used a commercial SPR imaging instrument (IBIS MX96) with 96 detection spots that were functionalized with RBD via amino-coupling. A sandwich assay with antibodies against IgG, IgM, and IgA was used to detect IgG, IgM, and IgA antibodies in diluted blood serum (1:100). It was demonstrated that serum samples from SARS-CoV-2 patients contained levels of all antibodies higher than healthy controls. A commercial prism-based SPR biosensor iCluebio was used to detect neutralizing antibodies against RBD in human blood plasma samples (Lee et al., 2023). A sensor surface, modified with hydrogel nanoparticles, was functionalized with RBD. The binding of the antibodies at the nM range was observed in buffers and plasma samples of vaccinated donors and controls. He et al. reported an LSPR imaging biosensor detecting interleukin 6 (IL-6) levels to

monitor the immune status of SARS-CoV-2 patients (He et al., 2022). They used dark-field microscopy to measure the LSPR signal from gold nanorods functionalized with peptide-aptamers as a capture agent. Direct detection was shown to achieve an LOD of 4.6 pg/mL in blood serum samples. Costa dos Santos et al. reported an SPR biosensor for detecting IgM antibodies against the Hepatitis A virus (HAV) (dos Santos et al., 2021). They employed a commercial SPR system, SensiQ Pioneer, with a sensor surface functionalized with major HAV capsid protein VP1 via amino-coupling. The antibodies diluted in buffer down to 0.02 nM were directly detected. The biosensor was found to discriminate positive blood serum samples of subjects with acute hepatitis A from healthy controls.

5.2.6. Cell-secreted proteins

SPR biosensors have been used to monitor the secretion of proteins from cells to study the development and progression of diseases. Ma et al. used a label-free single-molecule pulldown technique to image proteins released from cells (Ma, G.Z. et al., 2022). HeLa cells were attached to the cover glass on the top of a fluidic channel, and the proteins released during the cell lysis were adsorbed to the gold layer situated on the bottom side of the channel (Fig. 3). In conjunction with the plasmonic imaging platform, this approach was used to monitor the adsorption events of individual proteins and protein complexes with sizes from several hundreds of kDa to several MDa. Park et al. used the dark-field LSPR biosensor to study the secretion of the transforming growth factor- β (TGF- β) from different human cells (Park et al., 2021). A sensing platform based on AuNPs functionalized with antibodies against TGF- β attached to an APTES-modified glass surface was used. TGF- β secreted from cells was directly detected. It was observed that the sensor responses for TGF- β solutions secreted from cancer cell lines were about five times higher than those from normal cells. Liu et al. reported a high-throughput biosensor for the detection of secretion of IL-2 protein from individual cancer cells (Liu et al., 2022). The system was based on an inverted microscope and microwell array with gold nanoholes functionalized with streptavidin and biotinylated antibody against IL-2. Solutions containing IL-2 at different concentrations were injected along

the sensor surface to establish the calibration curve, and an LOD of 45.7 pM was established for direct detection. The motorized stage was used to move between microwells containing individual cells, and the temporal profiles of secretion from 150 stimulated cells were obtained. Wu et al. used a prism-based SPR imaging biosensor to monitor the production of interferon gamma (IFN- γ) from CD4⁺T cells (Wu et al., 2018). Spots with attached antibodies against CD4⁺T cells and IFN- γ were prepared on a sensor surface with poly(OEGMA-co-HEMA)matrix. CD4⁺T cells from peripheral blood were captured on Ab-modified spots. The cells were stimulated by an injection of a solution containing ESAT-6 and CFP-10. The secreted IFN- γ was detected on the sensing spot downstream. The study revealed that the CD4⁺T-cells from tuberculosis patients produced measurable concentrations of IFN- γ while the CD4⁺T-cells from healthy controls did not generate a measurable sensor response.

5.3. Exosomes

In recent years, the interest in analyzing exosomes and exosomal cargo molecules using biosensors has emerged. Chen et al. (2021) used a laboratory SPR instrument to determine human epidermal growth factor receptor 2 (HER2)-positive exosomes obtained from breast cancer cells. A sensor surface was functionalized with a molecular aptamer beacon consisting of an aptamer sequence to bind HER2 protein and sequence forming G-quadruplex-hemin structure. Exosomes were extracted from blood serum samples via ultracentrifugation and captured by the immobilized aptamer sequence via HER2 protein, releasing the G-quadruplex-hemin structure. In the final step, the tyramide-AuNPs were injected along the sensor surface, and G-quadruplex-hemin structure catalytically activated tyramide. The activated tyramide-AuNPs bound to the proteins on the surface of exosomes via the tyramide-tyrosine reaction, enhancing the sensor response. The lowest detected concentration of HER2-positive exosomes was 10⁴ exosomes/mL. A significant increase in the concentration of HER2-positive exosomes was shown in samples obtained from patients with breast cancer compared to healthy controls. Picciolini et al. (2021) used a commercial SPR imaging instrument to study the exosomes derived from

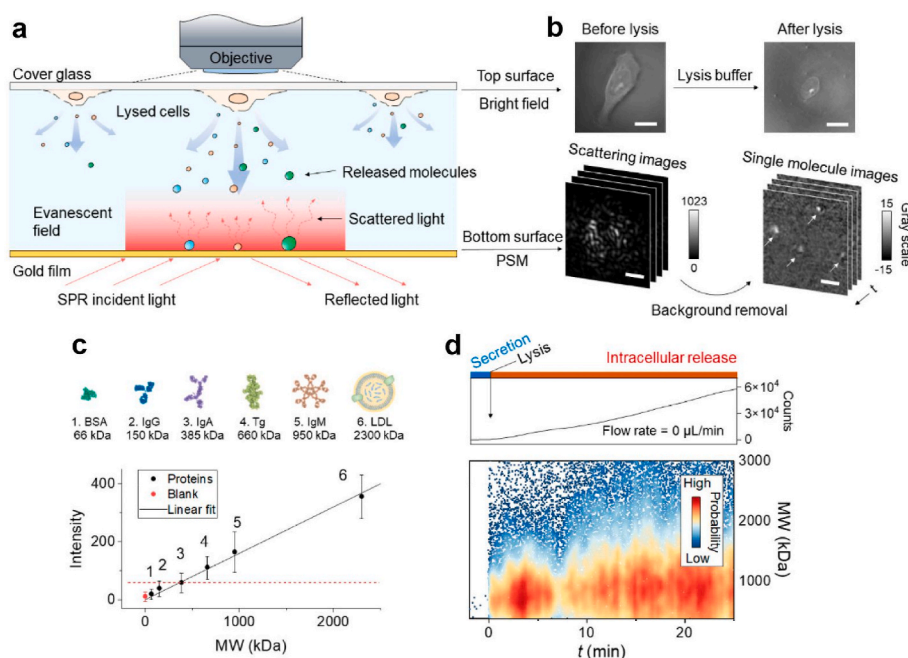


Fig. 3. SPR biosensor for the detection of individual cellular protein complexes. (a) Experimental design. (b) Bright field microscopy and SPR imaging showing the morphology of cells and adsorption of intracellular molecules, respectively. (c) Conversion from scattered light intensity to molecular weight of protein complexes. (d) Temporal profile of the release of intracellular molecules during cell lysis. Adapted with permission from (Ma, G.Z. et al., 2022). Copyright 2022 American Chemical Society.

central nervous system (CNS) cells in Alzheimer's disease. Antibodies and lectin covalently attached to the sensor surface were used to capture different CNS-derived exosomes that were extracted from blood plasma using size-exclusion chromatography. Translocator protein (TSPO), A β , and ganglioside M1 (GM1) on the surface of exosomes were further quantified using secondary antibodies. Elevated levels of CNS-derived exosomes, as well as increased expression of surface proteins, were found in the samples obtained from Alzheimer's disease patients when compared to healthy controls. Liao et al. used a commercial SPR platform to directly detect exosomes derived from the hepatic cancer cell line SMMC-7721 in spiked blood serum samples (Liao et al., 2020). The aptamer against the target exosomes was attached to a DNA tetrahedron structure immobilized on a sensor surface, followed by the direct capture of the exosomes in 50% serum. The sensor response was enhanced by the binding of polydopamine-AuNPs conjugated with CD63-specific aptamer, followed by the formation of gold precipitates from HAuCl₄ solution. The developed biosensor was evaluated for the detection of exosomes in spiked samples with an LOD of 5.6×10^5 exosomes/mL. Raghu et al. (2018) proposed an LSPR imaging (LSPRi) platform using gold nanostructures on quartz nanopillars for the detection of rare exosomal populations (Fig. 4). The authors used commercially available exosomes derived from breast adenocarcinoma cells as a model system. Antibody against surface marker CD63 was covalently attached to the gold nanostructures to capture the purified exosomes. The proposed system detected individual exosomes on an array of 10×10 nanopillars.

5.4. Viruses

Yang et al. used an LSPR biosensor to detect CoV NL63 coronavirus (Yang et al., 2022). A human angiotensin-converting enzyme 2 (ACE 2) was attached to silver nanotriangles via electrostatic and hydrophobic interactions. The biosensor was used to detect CoV NL63 coronavirus at concentrations $\sim 10^3$ - 10^4 PFU/mL in saliva samples. Chang et al. (2018) reported a prism-based SPR biosensor to detect avian influenza A H7N9 virus. A sensor surface was modified with anti-influenza antibody via amino-coupling, and the virus at levels $\sim 10^3$ - 10^5 copies/mL solution was directly detected in spiked nasal mucosa samples.

5.5. Bacteria

Nakano et al. used a prism-based SPR imaging sensor for O-antigen serotyping of *Escherichia coli* (Nakano et al., 2018). The selected sensor surface areas were modified with antibodies against specific serotypes, and the *E. coli* serotypes were directly detected with LODs of 1.1 – 17.6×10^6 CFU/mL. The developed SPR biosensor successfully identified 98.9% of 188 isolates obtained from patients suspected of harboring enterohemorrhagic *E. coli*. Gomez-Cruz et al. used a nanohole-based SPR imaging biosensor functionalized with antibody to detect uropathogenic

E. coli (Gomez-Cruz et al., 2018). *E. coli* was detected at 10^5 and 10^8 CFU/mL concentrations in urine samples.

5.6. Circulating tumor cells

Fathi et al. applied the commercial SPR biosensor BioNavis to detect cancer stem cells isolated from blood and bone marrow of acute myeloid leukemia (AML) patients (Fathi et al., 2019). Amino-coupling was used to functionalize a sensor surface with an antibody against CD133 transmembrane protein and the cells were captured at a concentration of 1×10^5 cells/mL. It was shown that the sensor responses to the capture of AML cells were higher than that for cells from a healthy control. Zhu et al. applied an SPR fiber sensor to detect MCF-7 breast cancer cells (Zhu et al., 2022). A sensor surface of a fiber was modified with antibodies against epithelial cell adhesion molecule (EpCAM). The MCF-7 cells were detected at 10^4 cells/mL in whole mouse blood.

5.7. Summary

SPR biosensors have been used to detect biomarkers in complex biological samples, such as blood serum and plasma, urine, saliva, and sputum (both diluted and undiluted).

Table 1 summarizes the characteristics of the reported works, including the studied pathology, selected biomarker, detection format, performance of the biosensor, and other relevant details. The collected data suggest that the most frequent targets of SPR biosensors are nucleic acids and proteins and that SPR biosensors enabled the detection of miRs and proteins down to sub-fM and low pg/mL levels, respectively. For large biological objects such as exosomes, bacteria, and CTCs, the reported LODs levels are 10^4 exosomes/mL, 10^6 CFU/mL, and 10^4 cells/mL, respectively. It is worth noting that the sensitive detection of large biological objects presents a challenge for surface-based biosensors, as the binding of such objects to the biorecognition elements on the surface of the sensor is affected by their slow diffusion from the liquid sample to the surface (Sheehan and Whitman, 2005). This issue can be mitigated by means of special microfluidic devices that improve mass transport towards the surface of the sensor (Lynn et al., 2013, 2015).

While the studies collected in Table 1 focus on demonstrating the feasibility of the SPR biosensor-based detection of medically relevant analytes (typically in a limited number of samples), there has been an increasing number of reports on the use of SPR biosensors in clinical studies involving cohorts from tens to hundreds of individuals (Table 2). Such reports were concerned with various diagnoses, such as oncological diseases (Agnihotri et al., 2020; Oldak et al., 2022a, 2022c; Prylutskiy et al., 2019; Sankiewicz et al., 2021; Singh et al., 2022), neuronal diseases (Bogdan et al., 2022; Górska et al., 2023; Pradhan et al., 2020), surgical interventions (Matuszczak et al., 2018a, 2018b), endometriosis (Warzecha et al., 2022), and burn injuries (Matuszczak et al., 2018c;

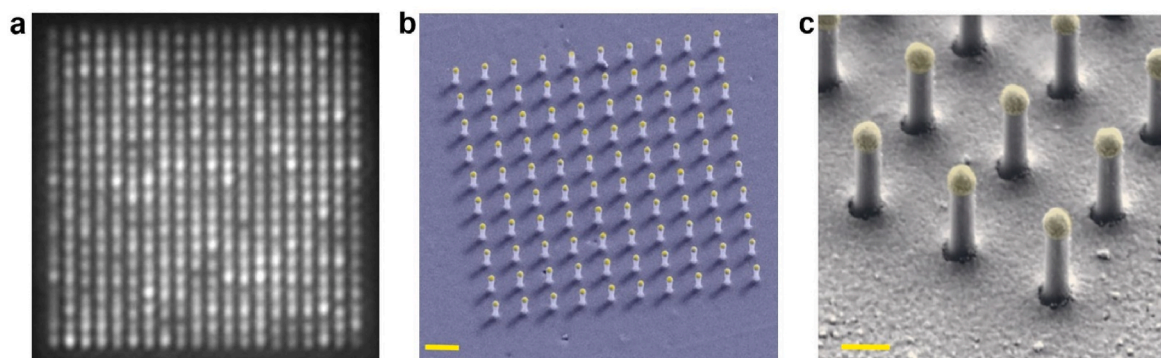


Fig. 4. (a) LSPRi image of a 20×20 array, each consisting of 100 nanopillars. (b) False colored SEM image of 10×10 nanopillar array (scale bar 1 μ m). (c) High-magnification false colored SEM image showing detailed view of individual nanopillars (scale bar 200 nm). Adapted with permission from (Raghu et al., 2018).

Table 1

Selected examples of applications of SPR biosensors developed for the detection of chemical and biological species.

Pathology	Biomarker	Detection format (detection time)	Performance of the biosensor ^{a,b}	Other clinically relevant details ^b	Ref.
RNA					
Multiple sclerosis	miR-422, miR-223, miR-126, miR-23a	SA: Ab-AuNPs (100 min)	LOD: 0.55 (miR-422), 0.88 (miR-223), 1.19 (miR-126), and 1.79 pM (miR-23a)	CS: C = 3 (total RNA isolates from blood serum)	Sguassero et al. (2019)
Diabetic nephropathy	miR-21, miR-192	SDA + SA: DNA-AuNPs (150 min)	LOD: 0.15 (miR-21), and 0.22 pM (miR-192)	RT: 103–110% (10% fetal bovine blood serum)	Wei et al. (2018)
Non-small cell lung cancer	miR-21, miR-378, miR-139, miR-200	SA: DNA-AgNCs + DNA-AuNPs (240 min)	MC: 2 fM - 20 nM	CS: P = 5, C = 5 (RNA isolated from exosomes from blood plasma); elevated in P	Wu et al. (2021)
Esophageal squamous cell carcinoma	miR-21, miR-155	SA: DNA-Fe ₃ O ₄ @AuNPs (120 min)	LOD: 502 (miR-21), and 483 fM (miR-155) (10% blood serum)	CC (10% blood serum)	Premaratne et al. (2019)
Myelodysplastic syndromes	miR-125b, miR-16	Release of specifically captured DNA-AuNPs (120 min)	LOD: 350 (miR-125b), and 550 aM (miR-16) (10% blood plasma)	CC (10% blood plasma)	Springer et al. (2021)
Glioma	miR-182	DNA walking system + SA: streptavidin	LOD: 620 aM	CS: P = 3, C = 3 (20% blood serum); elevated in P	Chen et al. (2022)
DNA					
Thalassemia	β-globin gene mutations	PCR + DD (15 min)	–	CS: P = 52, C = 19 (DNA isolates from blood or salivary swabs); P and C differentiation	Breveglieri et al. (2018)
Pneumocystis pneumonia	<i>Pneumocystis jirovecii</i> DNA	DD (15 min)	LOD: 2.1 nM	CS: P = 4, C = 8 (DNA isolated from sputum or bronchoalveolar lavage); P and C differentiation	Calvo-Lozano et al. (2020)
Colorectal cancer	RAS ctDNA	SA: DNA-AuNPs (80 min)	LOC: 2 ng/mL (10% blood plasma)	CS: P = 4, C = 4 (10% blood plasma); P and C differentiation	D'Agata et al. (2020)
Colorectal cancer	KRAS ctDNA	SA: DNA-AuNPs (120 min)	LOD: 1.45 ng/mL (10% blood plasma)	CS: P = 1, C = 1 (10% blood plasma); elevated in P	Bellassai et al. (2021)
Pancreatic cancer	KRAS ctDNA	DD (5 min)	LOC: 25 ng/mL (100% blood serum)	–	Tadimety et al. (2021)
Proteins					
Colorectal cancer	hnRNP A1	SA: Ab (70 min)	LOD: 0.22 nM	RT: ~15% (blood plasma)	Lee et al. (2020)
Myeloma	IL-2, sIL-2Rα	DD (1 min)	LOC: 20 nM	CS: P = 2, C = 2 (0.1% blood serum); elevated in P	Yang et al. (2021)
Bladder cancer	NMP22, CFH, HA	SA: Ab-AuNPs (120 min)	MC: 0.001–1000 ng/mL	RT: 80–120% (10% fetal bovine serum)	Yang et al. (2023)
Breast cancer	CA 15-3, CA 125, CEA, ErbB2	SA: Ab (90 min)	LOD: 1.85 (CA 15-3), 1021 U/mL (CA 125), and 76.19 (CEA), 31.9 ng/mL (ErbB2) (blood serum)	RT: 77–126% (100% blood serum)	Yavas et al. (2018)
Myelodysplastic syndromes	misfolded proteins	DD (1 min)	–	CS: P = 45, C = 16 (10% blood serum); elevated in P	Pastva et al. (2019)
Small cell lung cancer	NSE	DD (5 min)	LOD: 15.6 nM (1% blood serum)	CC (1% blood serum)	Sun et al. (2021)
Acute myocardial infarction	TnT	DD (2 min)	LOD: 14.8 nM	–	Palladino et al. (2018)
Heart failure	BNP	SA: Ab-MNPs + DNA-AuNPs (10 min)	MC: 0.1 pg/mL - 10 ng/mL	RT: 92–114% (100% blood serum)	Zhao et al. (2019)
Alzheimer's disease	Aβ ₁₋₄₀ , Aβ ₁₋₄₂ , τ	DD (60 min)	MC: 10 fM - 100 nM (blood plasma)	CC: blood plasma	Kim, H. et al. (2018)
Alzheimer's disease	τ	DD (60 min)	MC: 10 fM - 100 nM (blood plasma)	CS: P = 5, C = 1 (blood plasma); elevated in P	Kim et al. (2019)
Alzheimer's disease	Aβ ₁₋₄₂	DD (5 min)	MC: 2 fg/mL - 400 ng/mL	–	Nangare and Patil (2022)
Multiple sclerosis	Ab(GA ₁ , GM ₁ , GT _{1b})	DD (30 min)	LOD: 17.6 (GA ₁), 11.3 (GM ₁), and 8.2 ng/mL (GT _{1b}) (GT _{1b} : 2.34 ng/mL in 10% blood serum)	cross-reactivity (10% blood serum)	Malinick et al. (2020)
Neurodevelopmental disorders	SCG2	SA: HRP-streptavidin/Ab (150 min)	LOD: 0.016 ng/mL (10% blood serum)	CS: P = 8, C = 5 (10% blood serum); elevated in P	Lim et al. (2021)
Acute kidney injury	NGAL, IL-18, RBP	SA: Ab-MNPs (45 min)	LOD: 0.19 (NGAL), 0.51 (IL-18) and 0.7 ng/mL (RBP) (50% urine)	CS: P = 2, C = 1 (50% urine); elevated in P	Zhang et al. (2022)
Nephrotic syndrome	HSA, kappa, lambda, B2M	DD (5 min)	LOC: 0.36 (HSA), 0.05 (kappa), 0.1 (lambda), and 0.04 µg/mL (B2M)	CS: P = 7, C = 5 (0.1–10% urine); elevated in P	Zhang, L.L. et al. (2022)
Peanut allergy	allergen-specific IgE	SA: Ab-MNPs (10 min)	LOD: 5 pg/mL (diluted calf serum)	CS: P = 19, C = 13 (0.01–0.1% blood serum); elevated in P	Shen et al. (2018)
Celiac disease	GIP	Indirect competitive assay (10 min)	LOD: 1.6 ng/mL (100% urine)	RT (n = 21): 96–101% (100% urine)	Pelaez et al. (2020a)
Dengue fever	NS1	DD (10 min)	MC: 0.08–800 nM	CS: P = 16, C = 10 (1% blood plasma); elevated in P	Widoretto et al. (2020)
COVID-19	S1 spike protein	DD (10 min)	LOD: 0.26 nM	RT: 95 ± 18% (1% saliva)	Lewis et al. (2021)
COVID-19	S proteins of Alpha, Beta, and Gamma SARS-CoV-2	DD (20 min)	MC: 100 fM - 100 nM (blood serum)	CC (blood serum)	Bhalla et al. (2022)

(continued on next page)

Table 1 (continued)

Pathology	Biomarker	Detection format (detection time)	Performance of the biosensor ^{a,b}	Other clinically relevant details ^b	Ref.
Tuberculosis	HspX	DD (20 min)	LOD: 0.6 ng/mL (50% sputum)	CS: P = 12, C = 22 (50% sputum); elevated in P	Pelaez et al. (2020b)
COVID-19	Ab (SARS-CoV-2 S protein)	DD (20 min)	LOD: 0.1 ng/mL	RT: 80–95% (0.1% blood plasma)	Funari et al. (2020)
COVID-19	Ab (SARS-CoV-2 S protein)	SA: Ab (60 min)	LOD: 1.35 ng/mL	–	Qu et al. (2022)
COVID-19	Ab (SARS-CoV-2 RBD and S protein)	DD (30 min)	LOD: 21.1 (Ab(RBD)), and 86 ng/mL (Ab(N)) (10% blood serum)	CS: P = 100, C = 20 (10% blood serum); elevated in P	Calvo-Lozano et al. (2022)
COVID-19	IgG, IgM, IgA Abs (SARS-CoV-2 RBD protein)	SA: Ab (30 min)	–	CS: P = 53, C = 49 (1% blood serum); elevated in P	Schasfoort et al. (2021)
COVID-19	Ab (SARS-CoV-2 S protein)	DD (2 min)	LOC: 10 nM	CS: P = 13 (vaccinated donors), C = 3 (10% blood plasma); elevated in P	Lee et al. (2023)
COVID-19	IL-6	DD (30 min)	LOD: 4.6 pg/mL (blood serum)	CS: P = 7 (with treatment), C = 9 (without treatment) (blood serum); elevated in P	He et al. (2022)
Hepatitis A	Ab (HAV)	DD (10 min)	LOD: 20 pM	CS: P = 2, C = 5 (0.1% blood serum); elevated in P	dos Santos et al. (2021)
Breast and lung cancer	TGF- β	DD (30 min)	MC: 10 pg/mL to 100 μ g/mL	–	Park et al. (2021)
Lymphoma	IL-2	DD (50 min)	LOD: 45.7 pM	–	Liu et al. (2022)
Tuberculosis	IFN- γ	DD (5 min)	LOD: 50 pM	–	Wu et al. (2018)
Exosomes					
Breast cancer	HER2-positive exosomes	SA: tyramide-AuNPs (60 min)	LOC: 10 ⁴ exosomes/mL	CS: P = 8, C = 8 (exosomes isolated from blood serum); elevated in P	Chen et al. (2021)
Alzheimer's disease	CNS-derived exosomes	DD (20 min)	–	CS: P = 10, C = 10 (exosomes isolated from blood serum); elevated in P	Picciolini et al. (2021)
Hepatic cancer	SMMC-7721-derived exosomes	SA: DNA-AuNPs + HAuCl ₄ (100 min)	LOD: 5.6 \times 10 ⁵ exosomes/mL	RT: 95–104 % (50% blood plasma)	Liao et al. (2020)
Breast cancer	commercial MCF7-derived exosomes	DD (40 min)	Detection of individual exosome binding	–	Raghu et al. (2018)
Viruses					
COVID-19	CoV NL63 coronavirus	DD (2 h)	MC: 625 - 10 ⁴ PFU/mL (90% saliva)	CC (90% saliva)	Yang et al. (2022)
Avian influenza	influenza A H7N9 virus	DD (5 min)	MC: 10 ³ - 10 ⁵ copies/mL (10% nasal mucosa solution)	CC (10% nasal mucosa solution)	Chang et al. (2018)
Bacteria					
Hemolytic uremic syndrome	<i>E. coli</i>	DD (2 min)	LOD: 1.1 - 17.6 \times 10 ⁶ CFU/mL	Serotyping (correct identification of 186 from 188 isolates)	Nakano et al. (2018)
Urinary tract infection	<i>E. coli</i>	DD (15 min)	MC: 10 ⁵ and 10 ⁸ CFU/mL (urine)	CC (urine)	Gomez-Cruz et al. (2018)
CTCs					
Acute myeloid leukemia	AML cancer stem cells	DD (5 min)	LOC: 1 \times 10 ⁵ cells/mL	CS: P = 7, C = 1 (isolates from blood or bone marrow); elevated in P	Fathi et al. (2019)
Breast cancer	MCF-7 breast cancer cells	DD (15 min)	LOC: 10 ⁴ cells/mL (whole mouse blood)	–	Zhu et al. (2022)

^a Determined in buffer unless otherwise stated.

^b Concentration of complex sample written if known.

Abbreviations: Ab - antibody, SA - sandwich assay, DD - direct detection, AuNPs - gold nanoparticles, MNPs - magnetic nanoparticles, HRP - horseradish peroxidase, LOD - limit of detection, LOC - lowest observed concentration, MC - measured concentrations, CS - clinical samples, P - patient's sample, C - control sample, RT - recovery test, CC - calibration curve.

Weremijewicz et al., 2018). It should be noted that in these clinical studies, a large number of clinical samples was routinely analyzed (>50), and several studies involved as many as about 200 samples (Agnihotri et al., 2020; Bogdan et al., 2022; Singh et al., 2022). It illustrates the progress in the applicability of SPR biosensors in medical diagnostics, as only a few studies that analyzed more than 50 clinical samples were performed before 2017, as reviewed in (Masson, 2017).

The analysis of a large number of samples was facilitated by the use of multichannel SPR instruments (SPR imaging biosensors were ~35% and 70% of the instruments used in the studies collected in Tables 1 and 2, respectively), illustrating the multiplexing capabilities of SPR biosensor technology (Bocková et al., 2019). The distinct sensing areas for the detection of multiple analytes were created by deposited metallic spots on glass substrates (Oldak et al., 2022b), microfluidic channels (Špringer et al., 2021; Yavas et al., 2018), and surface chemistry modifications (Chrastinová et al., 2019; Sguassero et al., 2019; Wu et al., 2018).

It is interesting to note that, although the development of advanced

detection formats has received a great deal of attention, in about 60 percent of studies focusing on biosensor development (Table 1) and in all clinical studies (Table 2), direct detection was used. Such a high share suggests that the advantages of direct detection, such as a simple procedure (no need for additional reagents such as secondary antibodies) and short assay time (typically from several to tens of minutes) are appreciated, particularly in the clinical studies, in which tens and hundreds of samples need to be analyzed quickly (~15 min per sample or less). However, direct detection may suffer from interferences from complex clinical samples. This drawback could be overcome using more sophisticated detection formats, such as sandwich assays (which amounted to 34 percent of studies focusing on biosensor development, Table 1) or multi-step assays. Such assays enable the detection of analytes at lower concentrations than direct detection; however, the improvements in the detection performance are accompanied by increased laboriousness and prolonged detection times (typically 1–2 h).

Blood-derived samples (plasma and serum) constituted the majority of the analyzed clinical samples; ~70% of the works focused on

Table 2
Selected examples of applications of SPR biosensors in clinical studies.

Pathology	Biomarker	Detection format (detection time)	Optical instrument	Other clinically relevant details ^b	Ref.
Head and neck squamous cell carcinoma	sHLA-G, IL-10, IFN- γ	DD	SPR biosensor (Biacore 3000)	CS: P = 120, C = 99 (serum 17%)	Agnihotri et al. (2020)
Brain glioma malignancy	LN-5, FN, COL IV in	DD (10 min)	SPR imaging	CS: P = 56, C = 48 (plasma 0.001–20%)	Oldak et al. (2022a)
Brain glioma malignancy	Cathepsin B, D, S	DD (10 min)	SPR imaging	CS: P = 57, C = 48 (plasma 10–20%)	Oldak et al. (2022c)
Breast cancer	Biogenic polyamines	DD (15 min)	SPR biosensor (Plasmonest)	CS: P = 21, C = 9 (serum)	Prylutskiy et al. (2019)
Breast cancer	LOX5, Rac1, Rac1b, p38 α , Y-182, LIMK1, T-508, cofilin1, S-3	DD	SPR biosensor (Biacore 3000)	CS: P = 148, C = 52 (1.25 % serum)	Singh et al. (2022)
Transitional cell carcinoma	20S proteasome, UCHL1	DD (15 min)	SPR imaging	CS: P = 82, C = 27 (10% serum and 100% urine)	Sankiewicz et al. (2021)
Alzheimer's disease	UCHL1	DD (10 min)	SPR imaging	CS: P = 110, C = 60 (serum 10%)	Bogdan et al. (2022)
Alzheimer's disease	FOXO3A	DD	SPR biosensor (Biacore 3000)	CS: P = 37, C = 12 (serum)	Pradhan et al. (2020)
Multiple sclerosis	UCHL1	DD (10 min)	SPR imaging	CS: P = 100, C = 46 (plasma 10–50%)	Górska et al. (2023)
Surgery - acute appendicitis	Cathepsin B, 20S proteasome	DD (10 min)	SPR imaging	CS: P = 42, C = 18 (plasma 50%)	Matuszczak et al. (2018a)
Surgery - acute appendicitis	UCHL1, 20S proteasome	DD (10 min)	SPR imaging	CS: P = 27, C = 18 (plasma 10%)	Matuszczak et al. (2018b)
Endometriosis	Fibronectin, collagen IV	DD	SPR imaging	CS: P = 49, C = 35 (plasma and peritoneal fluid)	Warzecha et al. (2022)
Pediatric burn patients	MMP-2, laminin-5, collagen type IV	DD (10 min)	SPR imaging	CS: P = 31, C = 18 (10% plasma)	Weremijewicz et al. (2018)
Moderate and major burns	Proteasome, UCHL1	DD (10 min)	SPR imaging	CS: P = 30, C = 18 (plasma 10%)	Matuszczak et al. (2018c)

For an explanation of abbreviations see the text under [Table 1](#).

biosensor development and ~90% of clinical studies, which reflects the importance of blood in current medical diagnostics. As blood-derived samples are highly complex, in most studies samples were diluted to concentrations of 10% or less. A similar observation was reported in (Masson, 2017). This suggests that a certain degree of dilution is preferred in SPR biosensor-based analysis of clinical samples, although this dilution also lowers the concentration of the analyte to be detected.

6. Conclusions

SPR biosensors have made great strides toward applications in medical diagnostics. They have been successfully employed for the detection and quantification of a broad range of analytes in biological samples, such as blood plasma and serum, urine, saliva, and sputum. SPR biosensors were shown to be able to detect analytes in both diluted and undiluted samples; nevertheless, the majority of studies utilized highly diluted samples to mitigate the effects of sample complexity, which limited the ability of SPR biosensors to detect low levels of analytes. While numerous studies demonstrated the use of SPR biosensors for the analysis of tens of clinical samples, studies involving hundreds of samples remain relatively rare. However, the number of clinical studies employing SPR biosensors has grown substantially in the last decade. Although this is an encouraging trend, the review suggests that SPR biosensors have not yet attained maturity allowing them to become routine tools in medical diagnostics. The study suggests that further developments in the SPR biosensor technology are needed, such as improvements in sensor instrumentation, functionalization coatings, and detection assays. The advances in SPR biosensor instrumentation need to aim at compact and portable devices enabling point-of-care testing outside specialized laboratories.

CRediT authorship contribution statement

Tomáš Springer: Writing – review & editing, Writing – original draft, Investigation, Conceptualization. **Markéta Bocková:** Writing – review & editing, Writing – original draft, Conceptualization. **Jiří Slabý:**

Writing – review & editing, Writing – original draft, Conceptualization. **Foozieh Sohrabi:** Writing – review & editing, Writing – original draft, Conceptualization. **Magdalena Čapková:** Writing – original draft. **Jiří Homola:** Writing – review & editing, Investigation, Conceptualization.

Declaration of competing interest

The authors declare that they have no known competing financial interests or personal relationships that could have appeared to influence the work reported in this paper.

Acknowledgment

This work was supported by the Czech Science Foundation (contract 20–23787X) and by the project National Institute for Cancer Research (Program EXCELES, ID Project No. LX22NPO5102) funded by the European Union – Next Generation EU. The authors also acknowledge the assistance provided by the Advanced Multiscale Materials for Key Enabling Technologies project, supported by the Ministry of Education, Youth, and Sports of the Czech Republic (Project No. CZ.02.01.01/00/22_008/0004558, Co-funded by the European Union). The graphical abstract was created in BioRender (Čapková, M. (2025) <https://BioRender.com/h78z533>).

Data availability

Data will be made available on request.

References

- Agnihotri, V., Gupta, A., Kumar, L., Dey, S., 2020. Serum sHLA-G: significant diagnostic biomarker with respect to therapy and immunosuppressive mediators in Head and Neck Squamous Cell Carcinoma. *Sci. Rep.* 10 (1), 3806.
- Akkilic, N., Liljeblad, M., Blaho, S., Holta, M., Hook, F., Geschwindner, S., 2019. Avidity-based affinity enhancement using nanoliposome-amplified SPR sensing enables low picomolar detection of biologically active neuregulin 1. *ACS Sens.* 4 (12), 3166–3174.

- Alanazi, N., Almutairi, M., Alodhayb, A.N., 2023. A review of quartz crystal microbalance for chemical and biological sensing applications. *Sens Imaging* 24 (1).
- Ansaryan, S., Liu, Y.-C., Li, X., Economou, A.M., Eberhardt, C.S., Jandus, C., Altug, H., 2023. High-throughput spatiotemporal monitoring of single-cell secretions via plasmonic microwell arrays. *Nat. Biomed. Eng.* 7 (7), 943–958.
- Baek, S.H., Song, H.W., Lee, S., Kim, J.E., Kim, Y.H., Wi, J.S., Ok, J.G., Park, J.S., Hong, S., Kwak, M.K., Lee, H.J., Nam, S.W., 2020. Gold nanoparticle-enhanced and roll-to-roll nanoimprinted LSPR platform for detecting interleukin-10. *Front. Chem.* 8, 8.
- Bellassi, N., D'Agata, R., Marti, A., Rozzi, A., Volpi, S., Allegretti, M., Corradini, R., Giacomini, P., Huskens, J., Spoto, G., 2021. Detection of tumor DNA in human plasma with a functional PLL-based surface layer and plasmonic biosensing. *ACS Sens.* 6 (6), 2307–2319.
- Belushkin, A., Yesilkoy, F., Altug, H., 2018. Nanoparticle-enhanced plasmonic biosensor for digital biomarker detection in a microarray. *ACS Nano* 12 (5), 4453–4461.
- Belushkin, A., Yesilkoy, F., Gonzalez-Lopez, J.J., Ruiz-Rodriguez, J.C., Ferrer, R., Fabrega, A., Altug, H., 2020. Rapid and digital detection of inflammatory biomarkers enabled by a novel portable nanoplasmonic imager. *Small* 16 (3), 11.
- Berini, P., 2009. Long-range surface plasmon polaritons. *Adv. Opt. Photon* 1 (3), 484–588.
- Bhalla, N., Payam, A.F., Morelli, A., Sharma, P.K., Johnson, R., Thomson, A., Jolly, P., Canfarotta, F., 2022. Nanoplasmonic biosensor for rapid detection of multiple viral variants in human serum. *Sens. Actuator B-Chem.* 365, 8.
- Bian, J., Xing, X., Zhou, S., Man, Z.Q., Lu, Z.D., Zhang, W.H., 2019. Patterned plasmonic gradient for high-precision biosensing using a smartphone reader. *Nanoscale* 11 (26), 12471–12476.
- Bocková, M., Slabý, J., Springer, T., Homola, J., 2019. Advances in surface plasmon resonance imaging and microscopy and their biological applications. *Annu. Rev. Anal. Chem.* 12 (1), 151–176.
- Bogdan, S., Puscion-Jakubik, A., Klimiuk, K., Socha, K., Kochanowicz, J., Gorodkiewicz, E., 2022. UCHL1 and proteasome in blood serum in relation to dietary habits, concentration of selected antioxidant minerals and total antioxidant status among patients with Alzheimer's disease. *J. Clin. Med.* 11 (2).
- Breveglia, G., D'Aversa, E., Gallo, T.E., Pellegatti, P., Guerra, G., Cosenza, L.C., Finotti, A., Gambari, R., Borgatti, M., 2018. A novel and efficient protocol for Surface Plasmon Resonance based detection of four beta-thalassemia point mutations in blood samples and salivary swabs. *Sens. Actuator B-Chem.* 260, 710–718.
- Cai, J.X., Zhang, C.P., Liang, C.W., Min, S.Y., Cheng, X., Li, W.D., 2019. Solution-processed large-area gold nanochain-based metasurfaces on flexible plastics for plasmonic biomolecular sensing. *Adv. Opt. Mater.* 7 (19), 9.
- Califf, R.M., 2018. Biomarker definitions and their applications. *Exp. Biol. Med.* 243 (3), 213–221.
- Calvo-Lozano, O., Avino, A., Friaza, V., Medina-Escuela, A., Huertas, C.S., Calderon, E.J., Eritja, R., Lechuga, L.M., 2020. Fast and accurate pneumocystis pneumonia diagnosis in human samples using a label-free plasmonic biosensor. *Nanomaterials* 10 (6), 18.
- Calvo-Lozano, O., Sierra, M., Soler, M., Estevez, M.C., Chiscano-Camon, J., Ruiz-Sanmartin, A., Ruiz-Rodriguez, J.C., Ferrer, R., Gonzalez-Lopez, J.J., Esperalba, J., Fernandez-Naval, C., Bueno, L., Lopez-Aladid, R., Torres, A., Fernandez-Barat, L., Attoumani, S., Charrel, R., Coutard, B., Lechuga, L.M., 2022. Label-free plasmonic biosensor for rapid, quantitative, and highly sensitive COVID-19 serology: implementation and clinical validation. *Anal. Chem.* 94 (2), 975–984.
- Cetin, A.E., Kocer, Z.A., Topkaya, S.N., Yazici, Z.A., 2021. Handheld plasmonic biosensor for virus detection in field-settings. *Sens. Actuator B-Chem.* 344, 11.
- Cetin, A.E., Topkaya, S.N., 2019. Photonic crystal and plasmonic nanohole based label-free biodetection. *Biosens. Bioelectron.* 132, 196–202.
- Chang, Y.F., Wang, W.H., Hong, Y.W., Yuan, R.F., Chen, K.H., Huang, Y.W., Lu, P.L., Chen, Y.H., Chen, Y.M.A., Su, L.C., Wang, S.F., 2018. Simple strategy for rapid and sensitive detection of avian influenza A H7N9 virus based on intensity-modulated SPR biosensor and new generated antibody. *Anal. Chem.* 90 (3), 1861–1869.
- Chen, J.S., Chen, P.F., Lin, H.T.H., Huang, N.T., 2020. A Localized surface plasmon resonance (LSPR) sensor integrated automated microfluidic system for multiplex inflammatory biomarker detection. *Analyst* 145 (23), 7654–7661.
- Chen, S.J., He, Y.H., Liu, L., Wang, J.X., Yi, X.Y., 2022. DNA walking system integrated with enzymatic cleavage reaction for sensitive surface plasmon resonance detection of miRNA. *Sci. Rep.* 12 (1), 8.
- Chen, W.Q., Li, Z.Y., Cheng, W.Q., Wu, T., Li, J., Li, X.Y., Liu, L., Bai, H.J., Ding, S.J., Li, X.M., Yu, X.L., 2021. Surface plasmon resonance biosensor for exosome detection based on reformative tyramine signal amplification activated by molecular aptamer beacon. *J. Nanobiotechnol.* 19 (1), 10.
- Chen, Z.X., Peng, Y.J., Cao, Y., Wang, H., Zhang, J.R., Chen, H.Y., Zhu, J.J., 2018. Light-driven nano-oscillators for label-free single-molecule monitoring of MicroRNA. *Nano Lett.* 18 (6), 3759–3765.
- Chrastinová, L., Pastva, O., Bocková, M., Lynn, N.S., Šácha, P., Hubálek, M., Suttner, J., Kotlíň, R., Štikarová, J., Hlaváčková, A., Pímková, K., Cermák, J., Homola, J., Dyr, J. E., 2019. A new approach for the diagnosis of myelodysplastic syndrome subtypes based on protein interaction analysis. *Sci. Rep.* 9, 10.
- D'Agata, R., Bellassi, N., Allegretti, M., Rozzi, A., Korom, S., Manicardi, A., Melucci, E., Pescarmona, E., Corradini, R., Giacomini, P., Spoto, G., 2020. Direct plasmonic detection of circulating RAS mutated DNA in colorectal cancer patients. *Biosens. Bioelectron.* 170.
- de Planell-Saguer, M., Rodicio, M.C., 2013. Detection methods for microRNAs in clinic practice. *Clin. Biochem.* 46 (10), 869–878.
- Dey, P., Fabri-Faja, N., Calvo-Lozano, O., Terborg, R.A., Belushkin, A., Yesilkoy, F., Fabrega, A., Ruiz-Rodriguez, J.C., Ferrer, R., Gonzalez-Lopez, J.J., Estevez, M.C., Altug, H., Pruneri, V., Lechuga, L.M., 2019. Label-free bacteria quantification in blood plasma by a bioprinted microarray based interferometric point-of-care device. *ACS Sens.* 4 (1), 52–60.
- dos Santos, G.M.C., Alves, C.R., Pinto, M.A., Leon, L.A.A., Souza-Silva, F., 2021. Detection of antibodies against hepatitis A virus (HAV) by a surface plasmon resonance (SPR) biosensor: a new diagnosis tool based on the major HAV capsid protein VP1 (SPR-HAVP1). *Sensors* 21 (9), 11.
- Fan, H.L., Huang, L.P., Li, R., Chen, M.Q., Huang, J.J., Xu, H., Hu, W.J., Liu, G.L., 2022. A nanoplasmonic portable molecular interaction platform for high-throughput drug screening. *Adv. Funct. Mater.* 32 (46), 12.
- Fan, Z.Y., Geng, Z.X., Fang, W.H., Lv, X.Q., Su, Y., Wang, S.C., Chen, H.D., 2020. Smartphone biosensor system with multi-testing unit based on localized surface plasmon resonance integrated with microfluidics chip. *Sensors* 20 (2), 13.
- Fathi, F., Rahbarghazi, R., Movassaghpour, A.A., Rashidi, M.R., 2019. Detection of CD133-marked cancer stem cells by surface plasmon resonance: its application in leukemia patients. *Bba-Gen Subjects* 1863 (10), 1575–1582.
- Funari, R., Chu, K.Y., Shen, A.Q., 2020. Detection of antibodies against SARS-CoV-2 spike protein by gold nanospikes in an opto-microfluidic chip. *Biosens. Bioelectron.* 169, 8.
- Gomez-Cruz, J., Nair, S., Manjarrez-Hernandez, A., Gavilanes-Parra, S., Ascanio, G., Escobedo, C., 2018. Cost-effective flow-through nanohole array-based biosensing platform for the label-free detection of uropathogenic *E. coli* in real time. *Biosens. Bioelectron.* 106, 105–110.
- Gordon, J.G., Ernst, S., 1980. Surface-plasmons as a probe of the electrochemical interface. *Surf. Sci.* 101 (1–3), 499–506.
- Górska, E., Tylicka, M., Hermanowicz, A., Matuszczak, E., Sankiewicz, A., Gorodkiewicz, E., Hermanowicz, J., Karpinska, E., Socha, K., Kochanowicz, J., Jakoniuk, M., Kaminska, J., Homsak, E., Koper-Lenkiewicz, O.M., 2023. UCHL1, besides leptin and fibronectin, also could be a sensitive marker of the relapsing-remitting type of multiple sclerosis. *Sci. Rep-Uk* 13 (1).
- Hackett, L.P., Ameen, A., Li, W.Y., Dar, F.K., Goddard, L.L., Liu, G.L., 2018. Spectrometer-free plasmonic biosensing with metal-insulator-metal nanocup arrays. *ACS Sens.* 3 (2), 290–298.
- He, J.C., Zhou, L., Huang, G.T., Shen, J.L., Chen, W., Wang, C.Y., Kim, A., Zhang, Z.Y., Cheng, W.Q., Dai, S.Y., Chen, P.Y., Ding, F., 2022. Enhanced label-free nanoplasmonic cytokine detection in SARS-CoV-2 induced inflammation using rationally designed peptide aptamer. *ACS Appl. Mater. Interfaces* 12.
- Homola, J., 2008. Surface plasmon resonance sensors for detection of chemical and biological species. *Chem. Rev.* 108 (2), 462–493.
- Homola, J., Dostálek, J., Jiang, S., Ladd, J., Lofas, S., McWhirter, A., Myszká, D.G., Navratilova, I., Piliarik, M., Štěpánek, J., Taylor, A., Vaisocherová, H., 2006. Surface Plasmon Resonance Based Sensors. Springer-Verlag, Berlin.
- Hsieh, H.Y., Luo, J.X., Shen, Y.H., Lo, S.C., Hsu, Y.C., Tahara, H., Fan, Y.J., Wei, P.K., Sheen, H.J., 2022. A nanofluidic preconcentrator integrated with an aluminum-based nanoplasmonic sensor for Epstein-Barr virus detection. *Sens. Actuator B-Chem.* 355, 10.
- Huang, Y.L., Sun, T., Liu, L., Xia, N., Zhao, Y.H., Yi, X.Y., 2021. Surface plasmon resonance biosensor for the detection of miRNAs by combining the advantages of homogeneous reaction and heterogeneous detection. *Talanta* 234, 7.
- Jatschka, J., Dathe, A., Csáki, A., Fritzsche, W., Stranik, O., 2016. Propagating and localized surface plasmon resonance sensing — a critical comparison based on measurements and theory. *Sens. Bio-Sens. Res.* 7, 62–70.
- Kim, H., Lee, J.U., Kim, S., Song, S., Sim, S.J., 2019. A nanoplasmonic biosensor for ultrasensitive detection of Alzheimer's disease biomarker using a chaotropic agent. *ACS Sens.* 4 (3), 595–602.
- Kim, H., Lee, J.U., Song, S., Kim, S., Sim, S.J., 2018. A shape-code nanoplasmonic biosensor for multiplex detection of Alzheimer's disease biomarkers. *Biosens. Bioelectron.* 101, 96–102.
- Kim, S., Lee, S., Lee, H.J., 2018. An aptamer-aptamer sandwich assay with nanorod-enhanced surface plasmon resonance for attomolar concentration of norovirus capsid protein. *Sens. Actuator B-Chem.* 273, 1029–1036.
- Klinghammer, S., Uhlig, T., Patrovsky, F., Bohm, M., Schutt, J., Putz, N., Baraban, L., Eng, L.M., Cuniberti, G., 2018. Plasmonic biosensor based on vertical arrays of gold nanoantennas. *ACS Sens.* 3 (7), 1392–1400.
- Kuo, C.W., Wang, S.H., Lo, S.C., Yong, W.H., Ho, Y.L., Delaunay, J.J., Tsai, W.S., Wei, P. K., 2022. Sensitive oligonucleotide detection using resonant coupling between Fano resonance and image dipoles of gold nanoparticles. *ACS Appl. Mater. Interfaces* 14 (12), 14012–14024.
- Lee, H.S., Seong, T.Y., Kim, W.M., Kim, I., Hwang, G.W., Lee, W.S., Lee, K.S., 2018. Enhanced resolution of a surface plasmon resonance sensor detecting C-reactive protein via a bimetallic waveguide-coupled mode approach. *Sens. Actuator B-Chem.* 266, 311–317.
- Lee, S.H., Park, Y.E., Lee, J.E., Lee, H.J., 2020. A surface plasmon resonance biosensor in conjunction with a DNA aptamer-antibody bioreceptor pair for heterogeneous nuclear ribonucleoprotein A1 concentrations in colorectal cancer plasma solutions. *Biosens. Bioelectron.* 154, 6.
- Lee, S.K., Yim, B., Park, J., Kim, N.G., Kim, B.S., Park, Y., Yoon, Y.K., Kim, J., 2023. Method for the rapid detection of SARS-CoV-2-neutralizing antibodies using a nanogel-based surface plasmon resonance biosensor. *ACS Appl. Polym. Mater.* 8.
- Lewis, T., Giroux, E., Jovic, M., Martic-Milne, S., 2021. Localized surface plasmon resonance aptasensor for selective detection of SARS-CoV-2 S1 protein. *Analyst* 146 (23), 7207–7217.
- Liang, Y.Z., Cui, W.L., Li, L.X., Yu, Z.Y., Peng, W., Xu, T., 2019. Large-scale plasmonic nanodisk structures for a high sensitivity biosensing platform fabricated by transfer nanoprinting. *Adv. Opt. Mater.* 7 (7), 10.
- Liao, G.F., Liu, X.F., Yang, X.H., Wang, Q., Geng, X.H., Zou, L.Y., Liu, Y.Q., Li, S.Y., Zheng, Y., Wang, K.M., 2020. Surface plasmon resonance assay for exosomes based

- on aptamer recognition and polydopamine-functionalized gold nanoparticles for signal amplification. *Microchim. Acta* 187 (4), 9.
- Lim, S.H., Sung, Y.J., Jo, N., Lee, N.Y., Kim, K.S., Lee, D., Kim, N.S., Lee, J., Byun, J.Y., Shin, Y.B., Lee, J.R., 2021. Nanoplasmonic immunosensor for the detection of SCG2, a candidate serum biomarker for the early diagnosis of neurodevelopmental disorder. *Sci. Rep.* 11 (1), 11.
- Liu, J.X., Hu, X.L., Hu, Y.X., Chen, P., Xu, H., Hu, W.J., Zhao, Y.T., Wu, P., Liu, G.L., 2023. Dual AuNPs detecting probe enhanced the NanoSPR effect for the high-throughput detection of the cancer microRNA21 biomarker. *Biosens. Bioelectron.* 225, 9.
- Liu, Y., Zhang, N., Li, P., Yu, L., Chen, S.M., Zhang, Y., Jing, Z.G., Peng, W., 2019. Low-cost localized surface plasmon resonance biosensing platform with a response enhancement for protein detection. *Nanomaterials* 9 (7), 10.
- Liu, Y.C., Ansaryan, S., Li, X.K., Arvelo, E.R., Altug, H., 2022. Real-time monitoring of single-cell secretion with a high-throughput nanoplasmonic microarray. *Biosens. Bioelectron.* 202, 9.
- Lofas, S., Malmqvist, M., Ronnberg, I., Stenberg, E., Liedberg, B., Lundstrom, I., 1991. Bioanalysis with surface-plasmon resonance. *Sens. Actuatur B-Chem.* 5 (1–4), 79–84.
- Lopez-Munoz, G.A., Ortega, M.A., Ferret-Minana, A., De Chiara, F., Ramon-Azcon, J., 2020. Direct and label-free monitoring of albumin in 2D fatty liver disease model using plasmonic nanogratings. *Nanomaterials* 10 (12), 11.
- Lynn, N.S., Bocková, M., Adam, P., Homola, J., 2015. Biosensor enhancement using grooved micromixers: Part II, experimental studies. *Anal. Chem.* 87 (11), 5524–5530.
- Lynn, N.S., Šířová, H., Adam, P., Homola, J., 2013. Enhancement of affinity-based biosensors: effect of sensing chamber geometry on sensitivity. *Lab Chip* 13 (7), 1413–1421.
- Ma, G.Z., Zhang, P.F., Zhou, X.Y., Wan, Z.J., Wang, S.P., 2022. Label-free single-molecule pulldown for the detection of released cellular protein complexes. *ACS Cent. Sci.* 8 (9), 1272–1281.
- Ma, Z.T., Lv, X.Q., Fang, W.H., Chen, H.D., Pei, W.H., Geng, Z.X., 2022. Au nanoparticle-based integrated microfluidic plasmonic chips for the detection of carcinoembryonic antigen in human serum. *ACS Appl. Nano Mater.* 5 (11), 17281–17292.
- Malinick, A.S., Lambert, A.S., Stuart, D.D., Li, B.C., Puente, E., Cheng, Q., 2020. Detection of multiple sclerosis biomarkers in serum by ganglioside microarrays and surface plasmon resonance imaging. *ACS Sens.* 5 (11), 3617–3626.
- Masson, J.F., 2017. Surface plasmon resonance clinical biosensors for medical diagnostics. *ACS Sens.* 2 (1), 16–30.
- Matuszczak, E., Komarowska, M., Tylicka, M., Debek, W., Gorodkiewicz, E., Tokarzewicz, A., Sankiewicz, A., Hermanowicz, A., 2018a. Determination of the concentration of cathepsin B by SPRI biosensor in children with appendicitis, and its correlation with proteasomes. *Adv. Clin. Exp. Med.* 27 (11), 1529–1534.
- Matuszczak, E., Sankiewicz, A., Debek, W., Gorodkiewicz, E., Milewski, R., Hermanowicz, A., 2018b. Immunoproteasome in the blood plasma of children with acute appendicitis, and its correlation with proteasome and UCHL1 measured by SPR imaging biosensors. *Clin. Exp. Immunol.* 191 (1), 125–132.
- Matuszczak, E., Weremijewicz, A., Komarowska, M., Sankiewicz, A., Markowska, D., Debek, W., Gorodkiewicz, E., Milewski, R., Hermanowicz, A., 2018c. Immunoproteasome in the plasma of pediatric patients with moderate and major burns, and its correlation with proteasome and UCHL1 measured by SPR imaging biosensors. *J. Burn Care Res.* 39 (6), 948–953.
- Mayer, K.M., Hafner, J.H., 2011. Localized surface plasmon resonance sensors. *Chem. Rev.* 111 (6), 3828–3857.
- Mehta, N., Sahu, S.P., Shaik, S., Devireddy, R., Gartia, M.R., 2021. Dark-field hyperspectral imaging for label free detection of nano-bio-materials. *WIREs Nanomed. Nanobiotechnology* 13 (1), e1661.
- Nair, S., Gomez-Cruz, J., Manjarrez-Hernandez, A., Ascanio, G., Sabat, R.G., Escobedo, C., 2020. Rapid label-free detection of intact pathogenic bacteria in situ via surface plasmon resonance imaging enabled by crossed surface relief gratings. *Analyst* 145 (6), 2133–2142.
- Nakano, S., Nagao, M., Yamasaki, T., Morimura, H., Hama, N., Iijima, Y., Shinomiya, H., Tanaka, M., Yamamoto, M., Matsumura, Y., Miyake, S., Ichiyama, S., 2018. Evaluation of a surface plasmon resonance imaging-based multiplex O-antigen serogrouping for *Escherichia coli* using eleven major serotypes of Shiga -toxin-producing *E. coli*. *J. Infect. Chemother.* 24 (6), 443–448.
- Nan, J.J., Zhu, S.J., Ye, S.S., Sun, W.H., Yue, Y., Tang, X.D., Shi, J.W., Xu, X.S., Zhang, J. H., Yang, B., 2020. Ultrahigh-sensitivity sandwiched plasmon ruler for label-free clinical diagnosis. *Adv. Mater.* 32 (2), 9.
- Nangare, S., Patil, P., 2022. Chitosan mediated layer-by-layer assembly based graphene oxide decorated surface plasmon resonance biosensor for highly sensitive detection of beta-amyloid. *Int. J. Biol. Macromol.* 214, 568–582.
- Nylander, C., Liedberg, B., Lind, T., 1982. Gas-detection by means of surface-plasmon resonance. *Sensor. Actuatur.* 3 (1), 79–88.
- Oldak, L., Chludzinska-Kasperuk, S., Milewska, P., Grubczak, K., Reszec, J., Gorodkiewicz, E., 2022a. Laminin-5, fibronectin, and type IV collagen as potential biomarkers of brain glioma malignancy. *Biomedicine* 10 (9).
- Oldak, L., Lesniewska, A., Zelazowska-Rutkowska, B., Latoch, E., Lukaszewski, Z., Krawczuk-Rybak, M., Gorodkiewicz, E., 2022b. An array SPRI biosensor for simultaneous VEGF-A and FGF-2 determination in biological samples. *Appl. Sci.-Basel* 12 (24), 14.
- Oldak, L., Milewska, P., Chludzinska-Kasperuk, S., Grubczak, K., Reszec, J., Gorodkiewicz, E., 2022c. Cathepsin B, D and S as potential biomarkers of brain glioma malignancy. *J. Clin. Med.* 11 (22).
- Palladino, P., Minunni, M., Scarano, S., 2018. Cardiac Troponin T capture and detection in real-time via epitope-imprinted polymer and optical biosensing. *Biosens. Bioelectron.* 106, 93–98.
- Park, J., Lee, S., Choi, J., Choi, I., 2021. Extra- and intracellular monitoring of TGF-beta using single immunoplasmonic nanoprobe. *ACS Sens.* 6 (5), 1823–1830.
- Pastva, O., Chrastinová, L., Bocková, M., Kotlíň, R., Suttar, J., Hlaváčková, A., Štikarová, J., Ceznerová, E., Čermák, J., Homola, J., Dyr, J.E., 2019. Hsp70 trap assay for detection of misfolded subproteome related to myelodysplastic syndromes. *Anal. Chem.* 91 (22), 14226–14230.
- Pelaez, E.C., Estevez, M.C., Dominguez, R., Sousa, C., Cebolla, A., Lechuga, L.M., 2020a. A compact SPR biosensor device for the rapid and efficient monitoring of gluten-free diet directly in human urine. *Anal. Bioanal. Chem.* 412 (24), 6407–6417.
- Pelaez, E.C., Estevez, M.C., Mongui, A., Menendez, M.C., Toro, C., Herrera-Sandoval, O. L., Robledo, J., Garcia, M.J., del Portillo, P., Lechuga, L.M., 2020b. Detection and quantification of HspX antigen in sputum samples using plasmonic biosensing: toward a real point-of-care (POC) for tuberculosis diagnosis. *ACS Infect. Dis.* 6 (5), 1110–1120.
- Picciolini, S., Gualerzi, A., Carlomagno, C., Cabinio, M., Sorrentino, S., Baglio, F., Bedoni, M., 2021. An SPRI-based biosensor pilot study: analysis of multiple circulating extracellular vesicles and hippocampal volume in Alzheimer's disease. *J. Pharm. Biomed. Anal.* 192, 9.
- Portela, A., Calvo-Lozano, O., Estevez, M.C., Escuela, A.M., Lechuga, L.M., 2020. Optical nanogap antennas as plasmonic biosensors for the detection of miRNA biomarkers. *J. Mater. Chem. B* 8 (19), 4310–4317.
- Pradhan, R., Yadav, S.K., Prem, N.N., Bhagel, V., Pathak, M., Shekhar, S., Gaikwad, S., Dwivedi, S.N., Bal, C.S., Dey, A.B., Dey, S., 2020. Serum FOXO3A: a ray of hope for early diagnosis of Alzheimer's disease. *Mech. Ageing Dev.* 190.
- Premaratne, G., Dharmaratne, A.C., Al Mubarak, Z.H., Mohammadparast, F., Andiappan, M., Krishnan, S., 2019. Multiplexed surface plasmon imaging of serum biomolecules: Fe3O4@Au Core/shell nanoparticles with plasmonic simulation insights. *Sens. Actuatur B-Chem.* 299, 8.
- Prylutskiy, M.P., Bilko, N.M., Starodub, N.F., 2019. Detection of biogenic polyamines in blood of patients with breast cancer. *Regul. Mech. Biosyst.* 10 (2), 257–263.
- Qu, J.H., Leirs, K., Maes, W., Imbrechts, M., Callewaert, N., Lagrou, K., Geukens, N., Lammertyn, J., Spasic, D., 2022. Innovative FO-SPR label-free strategy for detecting anti-RBD antibodies in COVID-19 patient serum and whole blood. *ACS Sens.* 7 (2), 477–487.
- Raghu, D., Christodoulides, J.A., Christophersen, M., Liu, J.L., Anderson, G.P., Robitaille, M., Byers, J.M., Raphael, M.P., 2018. Nanoplasmonic pillars engineered for single exosome detection. *PLoS One* 13 (8), 13.
- Sankiewicz, A., Guszcz, T., Gorodkiewicz, E., 2021. Application of SPRI biosensors for determination of 20S proteasome and UCH-L1 levels in the serum and urine of transitional bladder cancer patients. *Appl. Sci-Basel* 11 (17).
- Schasfoort, R.B.M., 2017. Handbook of Surface Plasmon Resonance. The Royal Society of Chemistry.
- Schasfoort, R.B.M., van Weperen, J., van Amsterdam, M., Parisot, J., Hendriks, J., Koerselman, M., Karperien, M., Mentink, A., Bennink, M., Krabbe, H., Terstappen, L., Mulder, A.H.L., 2021. Presence and strength of binding of IgM, IgG and IgA antibodies against SARS-CoV-2 during COVID-19 infection. *Biosens. Bioelectron.* 183, 4.
- Sguassero, A., Artiga, A., Morasso, C., Jimenez, R.R., Rapun, R.M., Mancuso, R., Agostini, S., Hernis, A., Abols, A., Line, A., Gualerzi, A., Picciolini, S., Bedoni, M., Rovaris, M., Gramatica, F., de la Fuente, J.M., Vanna, R., 2019. A simple and universal enzyme-free approach for the detection of multiple microRNAs using a single nanostructured enhancer of surface plasmon resonance imaging. *Anal. Bioanal. Chem.* 411 (9), 1873–1885.
- Sheehan, P.E., Whitman, L.J., 2005. Detection limits for nanoscale biosensors. *Nano Lett.* 5 (4), 803–807.
- Shen, M., Joshi, A.A., Vannam, R., Dixit, C.K., Hamilton, R.G., Kumar, C.V., Rusling, J.F., Pecuh, M.W., 2018. Epitope-Resolved detection of peanut-specific IgE antibodies by surface plasmon resonance imaging. *Chembiochem* 19 (3), 199–202.
- Shrivastav, A.M., Satish, L., Kushmaro, A., Shvalya, V., Cvelbar, U., Abdulhalim, I., 2021. Engineering the penetration depth of nearly guided wave surface plasmon resonance towards application in bacterial cells monitoring. *Sens. Actuatur B-Chem.* 345, 9.
- Singh, A.K., Batra, A., Upadhyaya, A.D., Gupta, S., Hareesh, K.P., Dey, S., 2022. Circulatory level of inflammatory cytoskeleton signaling regime proteins in cancer invasion and metastasis. *Front. Oncol.* 12.
- Slabý, J., Bocková, M., Homola, J., 2021. Plasmonic biosensor based on a gold nanostructure array for detection of microRNA related to myelodysplastic syndromes. *Sens. Actuatur B-Chem.* 347, 7.
- Špačková, B., Lynn, N.S., Slabý, J., Šířová, H., Homola, J., 2018. A route to superior performance of a nanoplasmonic biosensor: consideration of both photonic and mass transport aspects. *ACS Photonics* 5 (3), 1019–1025.
- Špačková, B., Wrobel, P., Bocková, M., Homola, J., 2016. Optical biosensors based on plasmonic nanostructures: a review. *Proc. IEEE* 104 (12), 2380–2408.
- Sperling, J.R., Macias, G., Neale, S.L., Clark, A.W., 2018. Multilayered nanoplasmonic arrays for self-referenced biosensing. *ACS Appl. Mater. Interfaces* 10 (40), 34774–34780.
- Springer, T., Krejčík, Z., Homola, J., 2021. Detecting attomolar concentrations of microRNA related to myelodysplastic syndromes in blood plasma using a novel sandwich assay with nanoparticle release. *Biosens. Bioelectron.* 194, 6.
- Springer, T., Song, X.C., Ermini, M.L., Lamačová, J., Homola, J., 2017. Functional gold nanoparticles for optical affinity biosensing. *Anal. Bioanal. Chem.* 409 (16), 4087–4097.
- Sun, L.L., Shen, K.M., Zhang, J.B., Wan, W.J., Cao, W.J., Wang, Z.J., Guo, C.Z., 2021. Aptamer based surface plasma resonance assay for direct detection of neuron specific enolase and progastrin-releasing peptide (31-98). *RSC Adv.* 11 (51), 32135–32142.

- Tadimety, A., Wu, Z.Q., Molinski, J.H., Beckerman, R., Jin, C.R., Zhang, L.R., Palinski, T. J., Zhang, J.X.J., 2021. Rational design of on-chip gold plasmonic nanoparticles towards ctDNA screening. *Sci. Rep-Uk* 11 (1).
- Tu, L., Huang, L., Wang, W.H., 2019. A novel micromachined Fabry-Perot interferometer integrating nano-holes and dielectrophoresis for enhanced biochemical sensing. *Biosens. Bioelectron.* 127, 19–24.
- Turgeon, M.L., 2015. Linne & Ringsrud's Clinical Laboratory Science - E-Book: the Basics and Routine Techniques. Elsevier Health Sciences.
- Warzecha, D., Zalecka, J., Manka, G., Kiecka, M., Lipa, M., Spaczynski, R., Piekarski, P., Banaszewska, B., Jakimiuk, A., Issat, T., Rokita, W., Młodawski, J., Szubert, M., Sieroszewski, P., Raba, G., Szczupak, K., Kluz, T., Kluza, M., Wielgos, M., Oldak, L., Lesniewska, A., Gorodkiewicz, E., Laudanski, P., 2022. Plasma and peritoneal fluid fibronectin and collagen IV levels as potential biomarkers of endometriosis. *Int. J. Mol. Sci.* 23 (24).
- Wei, X., Duan, X., Zhou, X., Wu, J., Xu, H., Min, X., Ding, S., 2018. A highly sensitive SPRi biosensing strategy for simultaneous detection of multiplex miRNAs based on strand displacement amplification and AuNP signal enhancement. *Analyst* 143 (13), 3134–3140.
- Weremijewicz, A., Matuszczak, E., Sankiewicz, A., Tylicka, M., Komarowska, M., Tokarzewicz, A., Debek, W., Gorodkiewicz, E., Hermanowicz, A., 2018. Matrix metalloproteinase-2 and its correlation with basal membrane components laminin-5 and collagen type IV in paediatric burn patients measured with Surface Plasmon Resonance Imaging (SPRI) biosensors. *Burns* 44 (4), 931–940.
- Widoretno, Sjahrurachman, A., Dewi, B.E., Lischer, K., Pratami, D.K., Flamandita, D., Sahlan, M., 2020. Surface plasmon resonance analysis for detecting non-structural protein 1 of dengue virus in Indonesia. *Saudi J. Biol. Sci.* 27 (8), 1931–1937.
- Willets, K.A., Van Duyn, R.P., 2007. Localized surface plasmon resonance spectroscopy and sensing. *Annu. Rev. Phys. Chem.* 58, 267–297. Volume 58, 2007.
- Wong, C.L., Olivo, M., 2014. Surface plasmon resonance imaging sensors: a review. *Plasmonics* 9 (4), 809–824.
- Wu, C.L., He, J.A., Li, B.A., Xu, Y.Q., Gu, D.Y., Liu, H.M., Zhao, D., Shao, C.P., 2018. Real-time monitoring of T-cell-secreted interferon-gamma for the diagnosis of tuberculosis. *Biotechnol. Biotechnol. Equip.* 32 (4), 993–998.
- Wu, W.W., Yu, X.L., Wu, J.L., Wu, T., Fan, Y.P., Chen, W.Q., Zhao, M., Wu, H.P., Li, X.M., Ding, S.J., 2021. Surface plasmon resonance imaging-based biosensor for multiplex and ultrasensitive detection of NSCLC-associated exosomal miRNAs using DNA programmed heterostructure of Au-on-Ag. *Biosens. Bioelectron.* 175, 8.
- Yang, H.M., Yim, B., Lee, B.H., Park, Y., Kim, Y.G., Kim, J., Yoo, D., 2021. New tool for rapid and accurate detection of interleukin-2 and soluble interleukin-2 receptor a in cancer diagnosis using a bioresponsive microgel and multivalent protein binding. *ACS Appl. Mater. Interfaces* 13 (29), 33782–33789.
- Yang, Y.J., Murray, J., Haverstick, J., Tripp, R.A., Zhao, Y.P., 2022. Silver nanotriangle array based LSPR sensor for rapid coronavirus detection. *Sens. Actuator B-Chem.* 359, 9.
- Yang, Z.Y., Chang, W.H., Chiu, Y.C., Lin, C.H., 2023. Noninvasive detection of bladder cancer markers based on gold nanomushrooms and sandwich immunoassays. *ACS Appl. Nano Mater.* 6 (7), 5557–5567.
- Yanik, A.A., Cetin, A.E., Huang, M., Artar, A., Mousavi, S.H., Khanikaev, A., Connor, J.H., Shvets, G., Altug, H., 2011. Seeing protein monolayers with naked eye through plasmonic Fano resonances. *Proc. Natl. Acad. Sci. USA* 108 (29), 11784–11789.
- Yavas, O., Acimovic, S.S., Garcia-Guirado, J., Berthelot, J., Dobosz, P., Sanz, V., Quidant, R., 2018. Self-calibrating on-chip localized surface plasmon resonance sensing for quantitative and multiplexed detection of cancer markers in human serum. *ACS Sens.* 3 (7), 1376–1384.
- Zhang, L., Guo, W.Q., Lv, C.R., Liu, X.M., Yang, M., Guo, M., Fu, Q.Y., 2023. Electrochemical biosensors represent promising detection tools in medical field. *Adv. Sens. Energy Mat.* 2 (4).
- Zhang, L.L., Wang, H.G., Zhang, H., Zhang, N.R., Zheng, X.M., Li, W.G., Qiu, X.B., Yu, D. L., 2022. Development of a portable multiplexed instrument for multi-proteins detection in human urine using surface plasmon resonance. *Sens. Actuator B-Chem.* 369, 8.
- Zhang, Q.W., Li, Y., Hu, Q.Q., Xie, R.F., Zhou, W.J., Liu, X.H., Wang, Y., 2022. Smartphone surface plasmon resonance imaging for the simultaneous and sensitive detection of acute kidney injury biomarkers with noninvasive urinalysis. *Lab Chip* 22 (24), 4941–4949.
- Zhao, J.L., Liang, D.L., Gao, S.W., Hu, X.J., Koh, K., Chen, H.X., 2019. Analyte-resolved magnetoplasmonic nanocomposite to enhance SPR signals and dual recognition strategy for detection of BNP in serum samples. *Biosens. Bioelectron.* 141, 6.
- Zhu, S.D., Xie, Z.M., Chen, Y.Z., Liu, S.Y., Kwan, Y.W., Zeng, S.W., Yuan, W., Ho, H.P., 2022. Real-time detection of circulating tumor cells in bloodstream using plasmonic fiber sensors. *Biosens. Bioelectron.* 12 (11).
- Zopf, D., Pittner, A., Dathe, A., Grosse, N., Csaki, A., Arstila, K., Toppari, J.J., Schott, W., Dontsov, D., Uhlrich, G., Fritzsche, W., Stranik, O., 2019. Plasmonic nanosensor array for multiplexed DNA-based pathogen detection. *ACS Sens.* 4 (2), 335–343.